RECENT RESULTS ON CALCULATIONS OF RESONANCE TRANSITIONS IN W XIV - XLV

G O'Sullivan, C Suzuki, T Kato, H A Sakaue, D Kato, K Sato, N Tamura, S Sudo, C.S. Harte , R D'Arcy, E. Sokell and J. White

University College Dublin, Belfield, Dublin 4, Ireland

National Institute for Fusion Science, 322-6 Oroshi-cho, Toki 509-5292, Japan

National Institute of Fusion Science, Toki, Japan 19th February 2010

Outline

Background and Previous work

Spectra of W recorded at NIFS

Calculations of Resonance Spectra

- Open 5p subshell spectra and continuum generation
- The special case of W XIV
- Open 4f subshell spectra
- Open 4d subshell spectra
- Open 4p subshell spectra

Effects of low density on spectral complexity

Comparisons and conclusions

Need for data on W

W will be a limiter material in ITER

- **Identify lines to be used for diagnostics**
- **Radiation losses from W limited useful operation of PLT and ORMAK in 1970s.**

Joint project of EU, Russia, USA Japan, China, South Korea

large radius	6.2 m
minor radius	2.0 m
elongation	1.9
volume	837 m³
tor. field	5.3 T
plasma	
current	15 MA
density	10^{20} m³
temperature	20 keV
aux. power	73 MW
fusion power	500 MW
pulse length	500 s

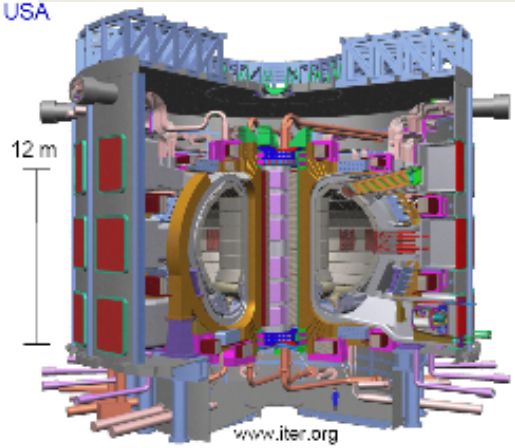

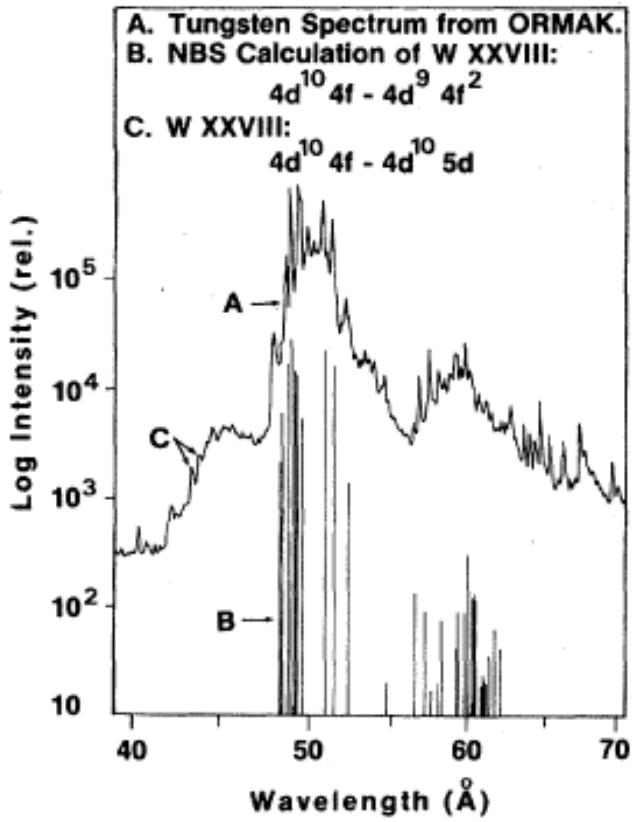

FIG. 2. Comparison of the calculated $4d^{10}4f$-$4d^{9}4f^{2}$ transition array (B) of W XXVIII with the tungsten spectrum (A) produced by ORMAK. It includes the identification of the $4^{10}4f$-$4d^{10}5d$ doublet (C).

Sugar & Kaufman PRA21,2096 (1980)

W^{21+-} W^{45+} Berlin EBIT Radke *et al* PRA64,012520, 2001

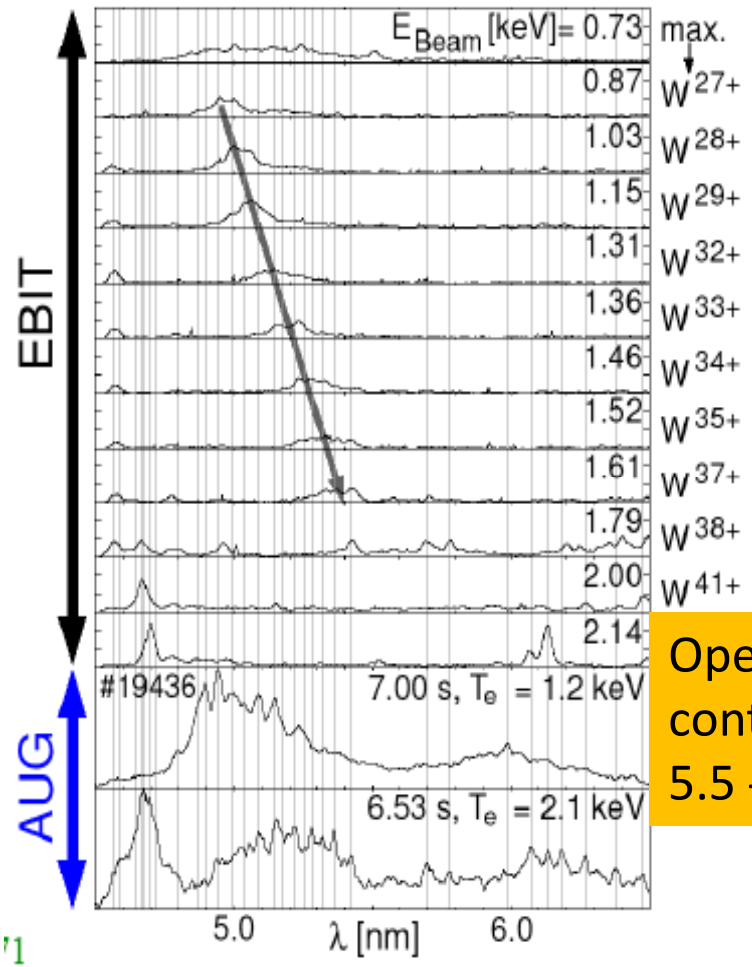

Th. Pütterich et al., J. Phys. B 38 (2005) 3071

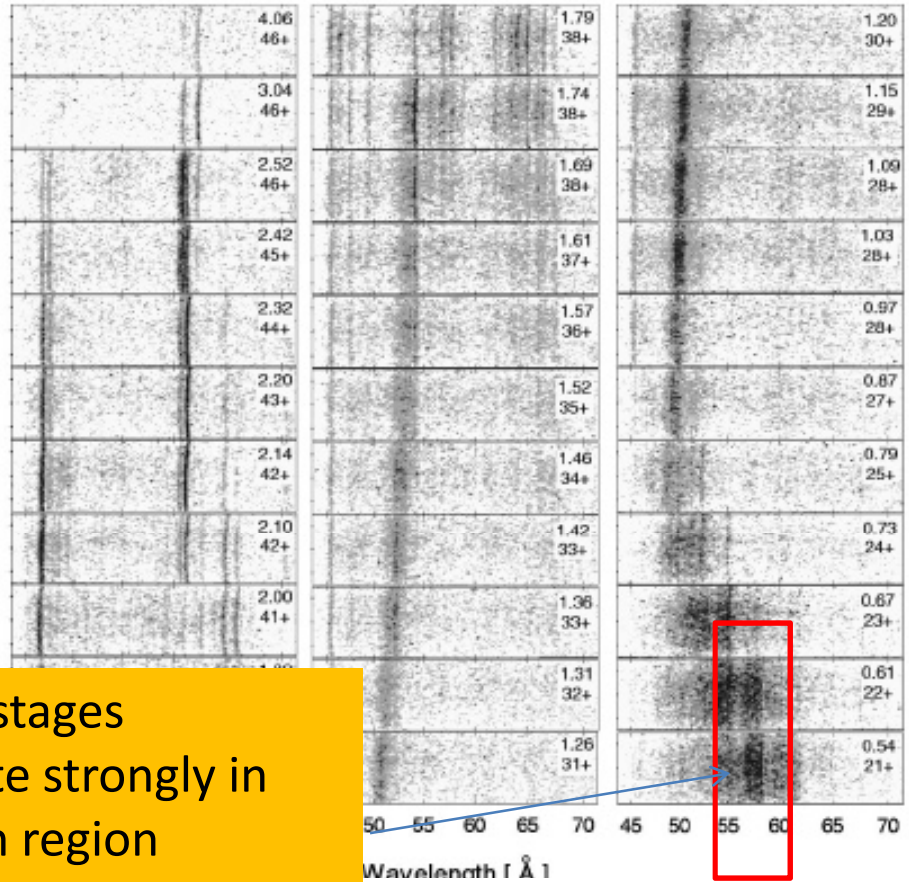

Open 4f stages contribute strongly in 5.5 -6 nm region

FIG. 1. Spectra from medium-charge-state ions of tungsten between 45 and 70 Å. The upper and lower labels plotted on the right side of each spectrum indicate the energy of the ionizing electron beam (in keV) and the highest allowed charge state of tungsten corresponding to the given value of E_{beam}.

Effects of Configuration Interaction

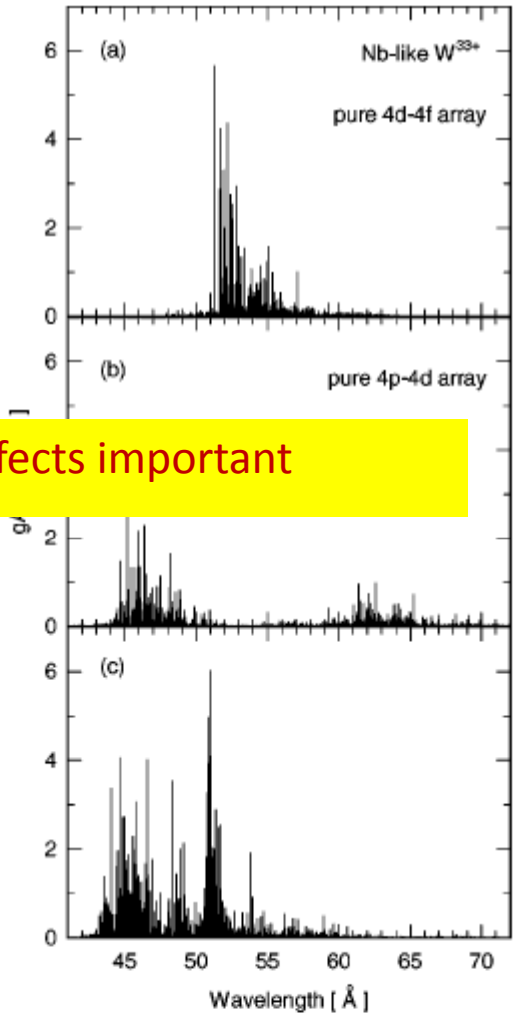

FIG. 3. gA distributions for transitions in Nb-like W^{33+}. In (a) and (b), the distributions for the pure $4p^6\,4d^5-4p^6\,4d^4\,4f$ and $4p^6\,4d^5-4p^5\,4d^6$ transition arrays are presented. (c) is a plot of the gA distribution for the mixed $4p^6\,4d^5-[4p^5\,4d^6+4p^6\,4d^4\,4f]$ array.

CI Effects important

Spectra from elements with Z > 50 contain an intense UTA (Unresolved Transition Array) due to $4p^64d^n$ - $4p^54d^{n+1}+4d^{n-1}4f$ ($0\leq n\leq 9$) transitions.

Configuration interaction (CI) causes transitions in adjacent ion stages to overlap in energy.

The UTA model predicts that for $4p^64d^n$ - $4d^{n-1}4f$ the position of the array peak should be at:

$$E = E_{av}(a) - E_{av}(b) + \delta E,$$

where

$$\delta E \sim 2(n-1)G^1(4d,4f)/9$$

CI between $4p^54d^{n+1}$ and $4d^{n-1}4f$ keeps it close to $2G^1(4d,4f)$ above $E_{av}(a) - E_{av}(b)$

(Mandelbaum et al PRA38, 12, 1987)

CI effects also cause a spectral narrowing, so the UTA have widths of ~ 5-10 eV. **W situation is complicated by spin orbit splitting of 4p and 4d.**

Unresolved Transition Arrays (UTA)

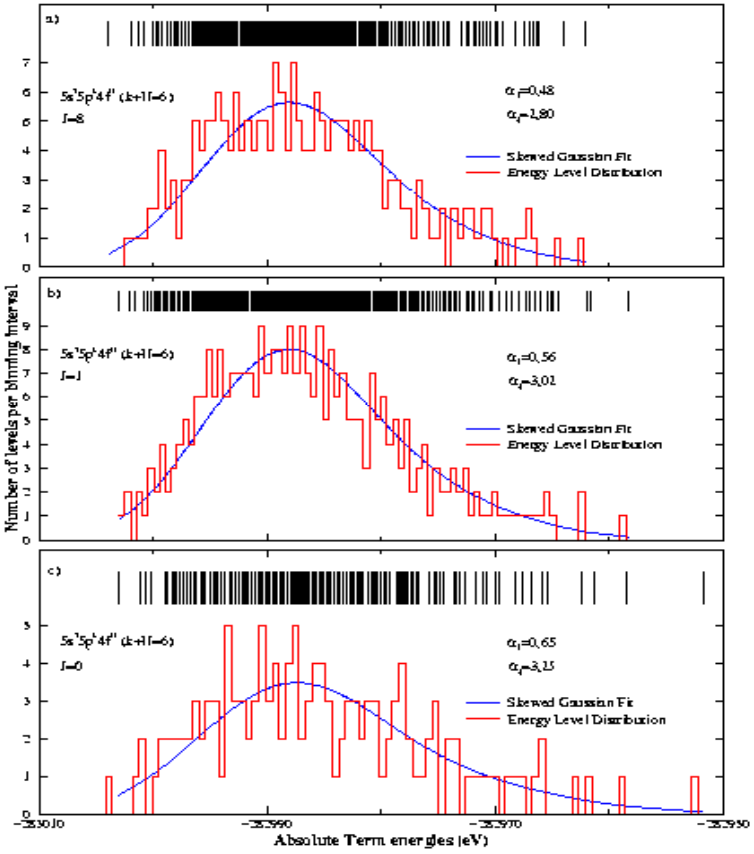

Figure 3.12: Skewed Gaussian Fits and Energy Level Distributions for a) $5s^2 5p^k 4f^N$ $(k+N=6)$ and J=8, b) $5s^2 5p^k 4f^N$ $(k+N=6)$ and J=1 and c) $5s^2 5p^k 4f^N$ $(k+N=6)$ and J=0.

- A UTA has too many lines to identify individual transitions.
- Energy level and spectral distributions can be parameterised statistically in terms of moments of the array *(Bauche, and Bauche-Arnoult Phys Scr **T40**, 58, 1992)*

- The n^{th} order centred moment is defined as:

$$\mu^c_n = [\Sigma_k \langle k \mid H \mid k \rangle - E_{av}]^n / g_k$$

where g_k is the statistical weight.

The width of an array = $2(2\ln \mu^c_2)^{1/2}$.

The skewness = $\mu^c_3 / \mu^c_2{}^{3/2}$ measures assymetry .

The kurtosis = $\mu^c_4 / \mu^c_2{}^2$ gives the shape.

Comparison of EBIT data with Calculations

Putterich et al *Plasma Phys. Control. Fusion* **50** 085016 2008

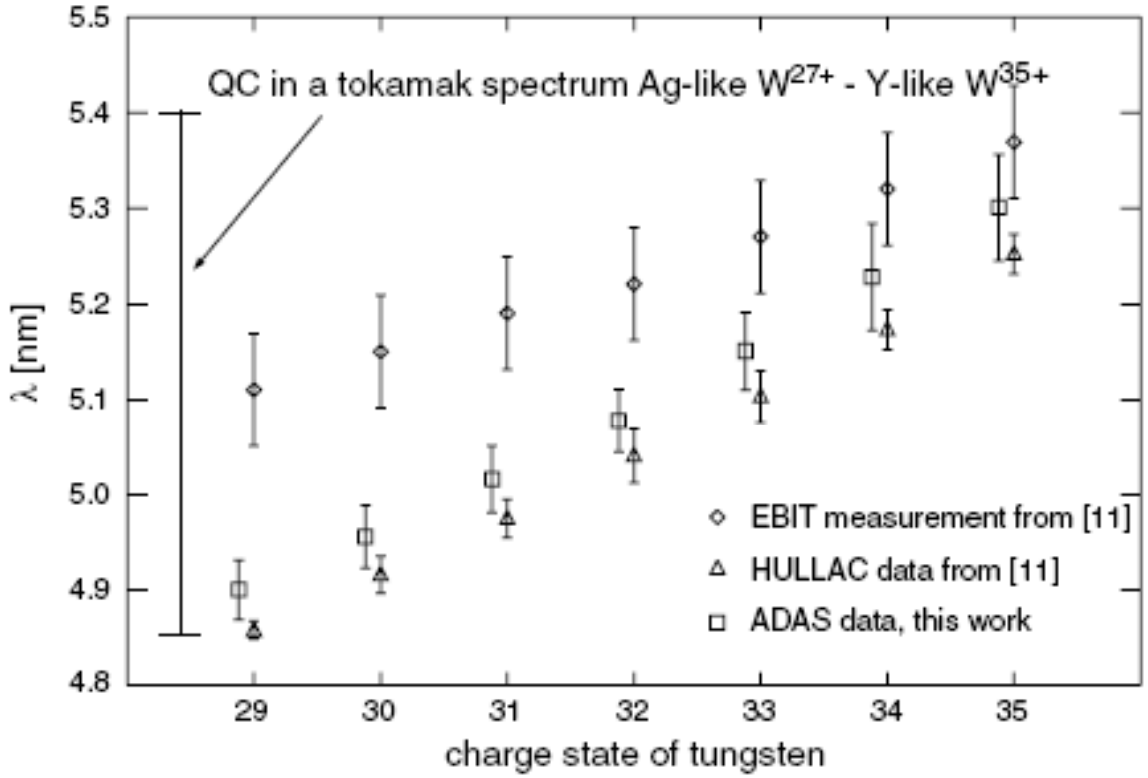

Figure 10. Wavelengths and spectral widths (indicated by bars) of the emissions responsible for the quasicontinuous structure around 5 nm from experiment and calculations. The ADAS data points (this work) have been displaced horizontally for better display.

Asdex-U data

Putterich et al *Plasma Phys. Control. Fusion* **50** 085016 2008

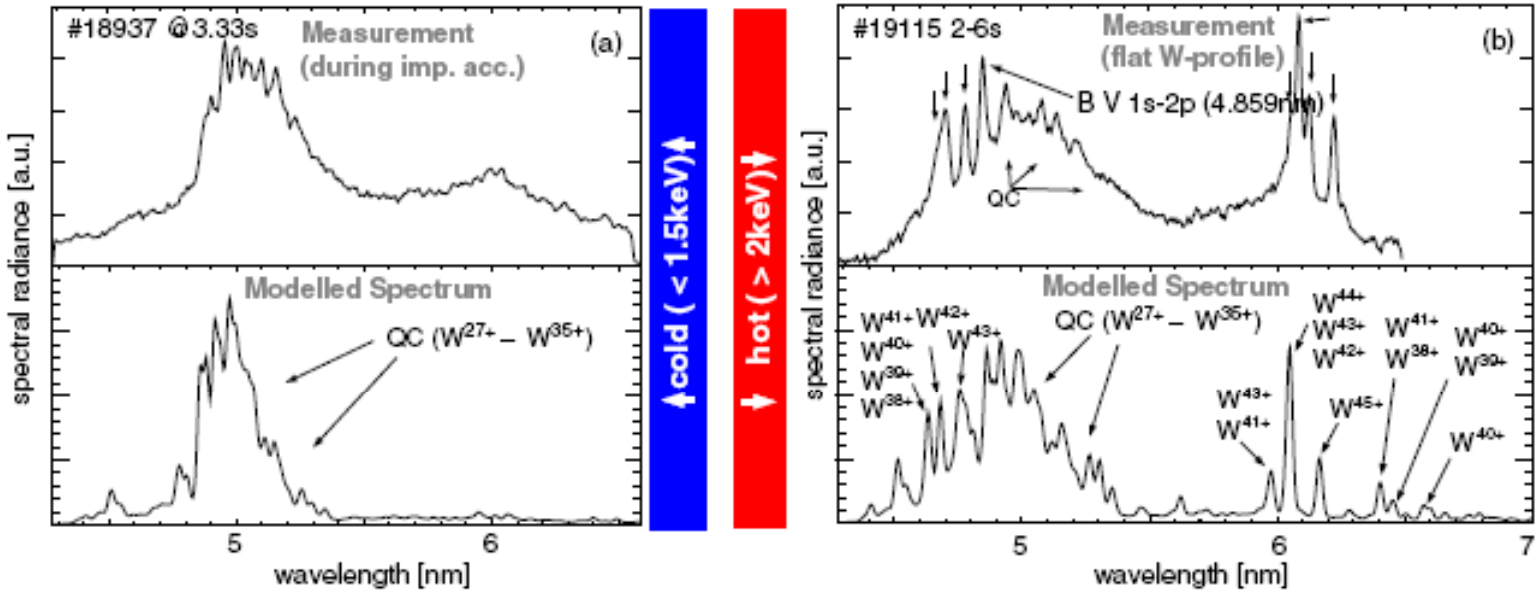

Figure 9. (*a*) Emissions of Ag-like W^{27+}–Y-like W^{35+} (grazing incidence spectrometer) during a discharge with impurity accumulation highlighting these ionization stages and modelled spectra using a peaked W profile. (*b*) Same spectral range at higher T_e and flat W profile, exhibiting additional spectral lines emitted by ionization stages up to W^{45+} and the corresponding modelling. The emissions depicted in part (*a*) are still visible because the LOS passes also through colder plasma at the plasma edge. Small arrows indicate the spectral lines used in section 2 for quantifying fractional abundances of ionization stages.

Asdex-U data (ctd.) Asmussen et al. *Nucl. Fusion* 38, 967, 1998

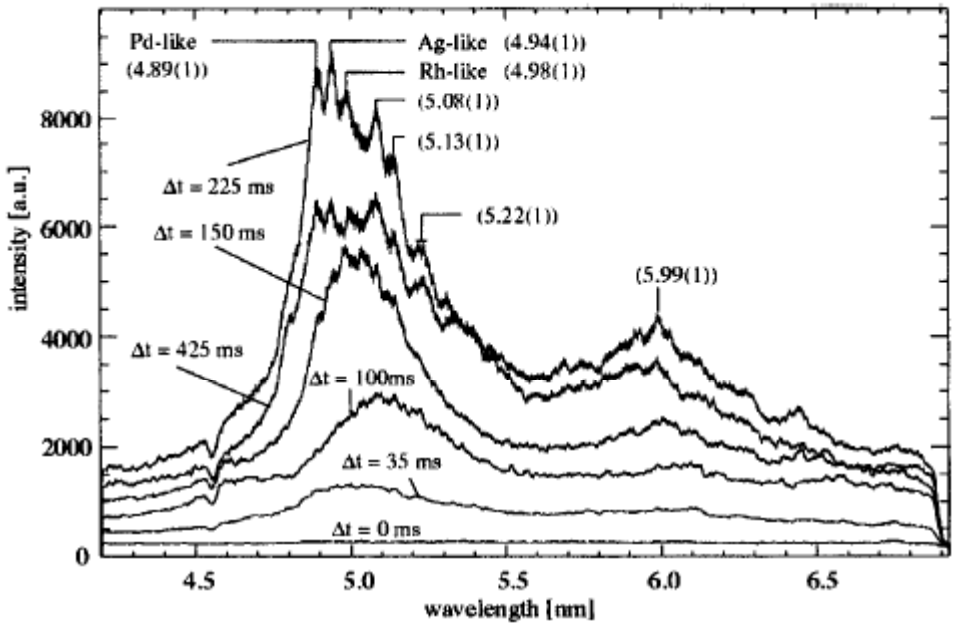

FIG. 3. Tungsten quasi-continuum in the 6 nm region from a plasma discharge with a central temperature of $T_{e,0} = 0.9$ keV after tungsten laser ablation (discharge 4955, $\bar{n}_e \approx 7 \times 10^{19}$ m^{-3}, $I_p = 1$ MA). Owing to accumulation effects the central tungsten radiation becomes very strong, causing a hollow T_e profile and a spreading of the region with silver-, palladium- and rhodium-like tungsten ions. This enables a clearer observation of the spectral lines of these ions.

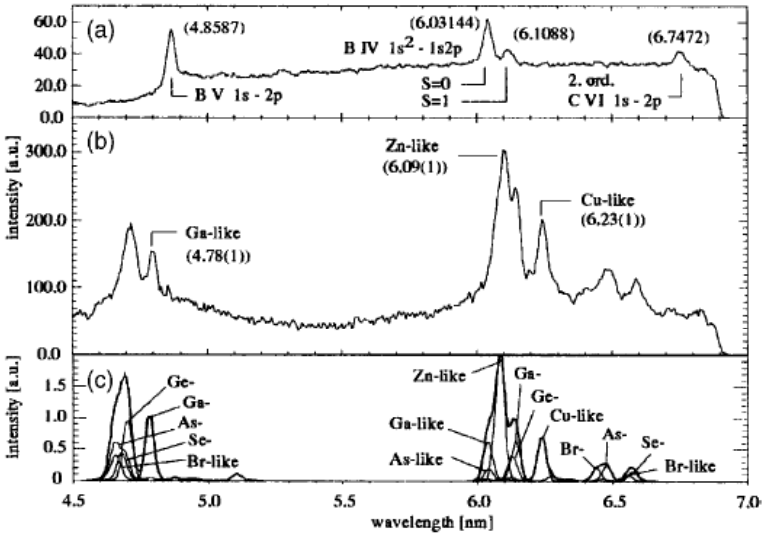

FIG. 5. Spectral lines of highly ionized tungsten in the 6 nm region: (a) measured background spectrum used for the wavelength calibration, (b) time integrated spectra with the background radiation subtracted ($t_{integ} = 100$ ms, 400 ms after tungsten injection, discharge 4896, 7 MW NBI, $\bar{n}_e \approx 8 \times 10^{19}$ m^{-3}, $T_{e,0} \approx 2.4$ keV, $I_p = 1$ MA), (c) calculated spectra (HULLAC code), the element symbols indicate isoelectronic sequences.

Outline

Background and Previous work

Spectra of W recorded at NIFS

Calculations of Resonance Spectra

- Open 5p subshell spectra and continuum generation
- The special case of W XIV
- Open 4f subshell spectra
- Open 4d subshell spectra
- Open 4p subshell spectra

Effects of low density on spectral complexity

Comparisons and conclusions

NIFS Results

Plasma Temperature close to 1.5 keV

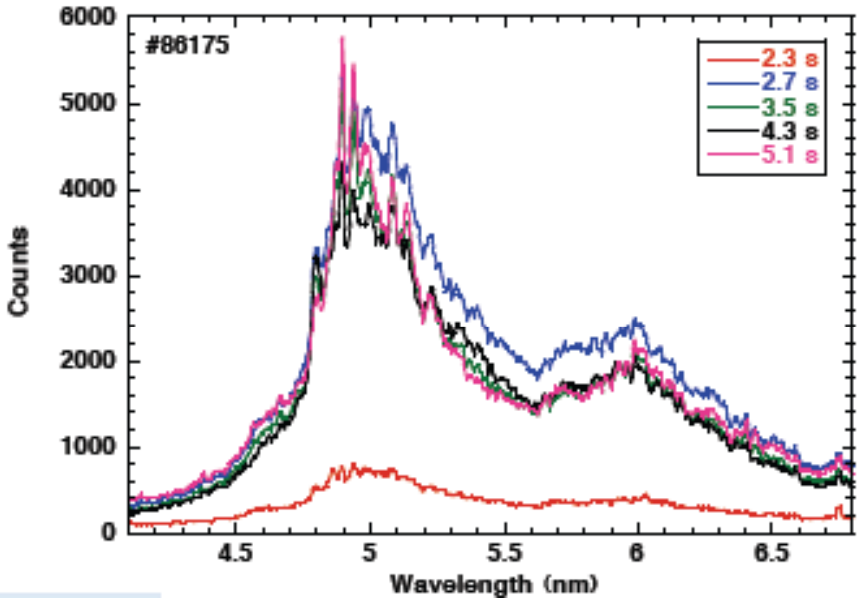

Plasma Temperature close to 3 keV

Main regions of difference

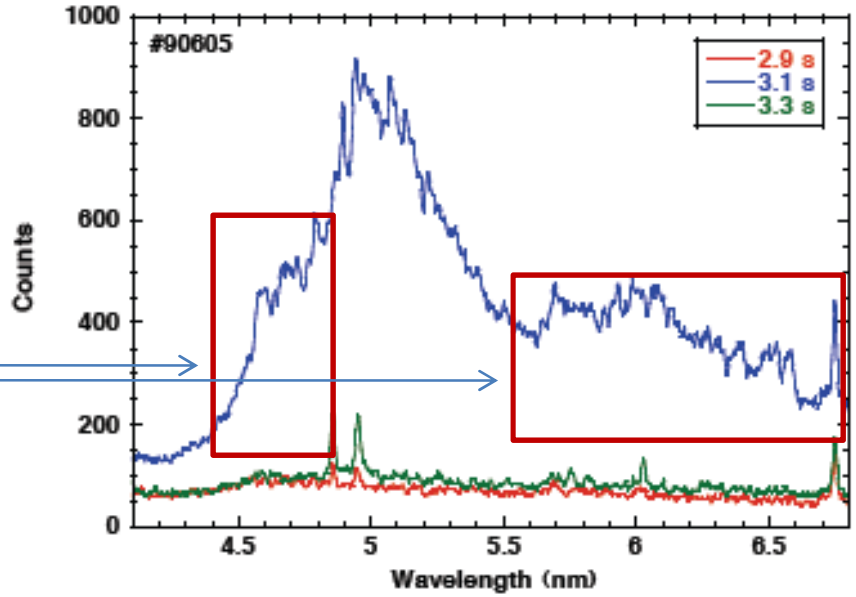

Outline

Background and Previous work

Spectra of W recorded at NIFS

Calculations of Resonance Spectra

- Open 5p subshell spectra and continuum generation
- The special case of W XIV
- Open 4f subshell spectra
- Open 4d subshell spectra
- Open 4p subshell spectra

Effects of low density on spectral complexity

Comparisons and conclusions

Method of Calculation

Cowan (Hartree Fock with Configuration Interaction) Code used.

Gives transition energies, gA values and oscillator strengths.

Can 'scale' Slater Condon parameters (Direct, F^k, Exchange, G^k and Spin-Orbit, ζ, Integrals – In LS Coupling $E_n = E_{AV} + \Sigma_k a_k F^k + \Sigma_k b_k G^k$).

F^k, G^k and R^k parameters reduced to 85%. Spin Orbit parameter unchanged
Accuracy generally within 1% (transition energies)

For $\delta n = 0$, transitions generally don't move much with ζ, where ζ is the effective charge (degree of ionisation + 1).

For $\delta n = 1$, transition energies (E_n) generally scale approximately according to $E_n \alpha \zeta^2$ where ζ is the effective charge (degree of ionisation + 1).
Spectral lines shift to shorter wavelengths along a sequence.

Important point to note:

Ground configurations frequently change along isoelectronic sequences because of level reordering by principal quantum number.

- In Ca I ground configuration is (Ar) $4s^2$, this changes to (Ar) $3d^2$.

- Hyperalkali ions: PmI: $4d^{10}5s^25p^66s^24f^5$ changes to $4d^{10}\,4f^{14}5s$ at the 15^{th} ion stage along the sequence *(Curtis and Ellis PRL 45, 2099 1989).* Confirmed earlier for 5s-5p doublet of Au XIX *(Träbert and Heckman Z. Phys 1, 381, 1986)*

- Xe sequence: transitions based on $5p^6$ vanish at Pr VI, ground configuration changes to $(5p4f)^6$.

Reason:

The effective radial potential is of the form:

$$-Z'e^2/4\pi\varepsilon_0 r + l(l+1)h^2/8\pi^2r^2$$

in neutrals and low ion stages the centrifugal term dominates and causes irregularities in filling of subshells. With increasing ionisation the Coulomb term becomes dominant.

Implications for tungsten:

Spectra of tungsten from W VII – W XVII are dominated by the effects of 4f contraction.

W VII Ground State : $4d^{10}5s^{2}5p^{6}4f^{14}\ {}^{1}S_{0}$ spectrum analysed (Sugar and Kaufman JOSA66, 1019 1976)

W VIII: Ground State (probably) : $4d^{10}5s^{2}5p^{6}4f^{13}$ but $4d^{10}5s^{2}5p^{5}4f^{14}$ only 800 cm^{-1} away (Carlson et al At. Data. Nuc. Data Tables 2, 63, 1970).

W IX: Ground State (probably) : $4d^{10}5s^{2}5p^{4}4f^{14}$ but $4d^{10}5s^{2}5p^{5}4f^{13}$ and $4d^{10}5s^{2}5p^{6}4f^{12}$ nearby. (Spread =25.18 eV)

W X: Ground State : $4d^{10}5s^{2}5p^{3}4f^{14}$ but $4d^{10}5s^{2}5p^{4}4f^{13}$, $4d^{10}5s^{2}5p^{5}4f^{12}$ and $4d^{10}5s^{2}5p^{6}4f^{11}$ nearby. (Spread = 47.07 eV)

W XI: Ground State : $4d^{10}5s^{2}5p^{2}4f^{14}$ but $4d^{10}5s^{2}5p^{3}4f^{13}$, $4d^{10}5s^{2}5p^{4}4f^{12}$, $4d^{10}5s^{2}5p^{5}4f^{11}$ and $4d^{10}5s^{2}5p^{6}4f^{10}$ nearby. (Spread = 95.59 eV)

W XII: Ground State : $4d^{10}5s^{2}5p^{1}4f^{14}$ but $4d^{10}5s^{2}5p^{2}4f^{13}$, $4d^{10}5s^{2}5p^{3}4f^{12}$, $4d^{10}5s^{2}5p^{4}4f^{11}$, $4d^{10}5s^{2}5p^{5}4f^{10}$, and $4d^{10}5s^{2}5p^{6}4f^{9}$ nearby. (Spread = 134.73)

W XIII: Ground State : $4d^{10}5s^{2}4f^{14}$ but $4d^{10}5s^{2}5p4f^{13}$, $4d^{10}5s^{2}5p^{2}4f^{12}$, $4d^{10}5s^{2}5p^{3}4f^{11}$, $4d^{10}5s^{2}5p^{4}4f^{10}$, $4d^{10}5s^{2}5p^{5}4f^{9}$ and $4d^{10}5s^{2}5p^{6}4f^{8}$ nearby. (Spread = 195.85 eV).

Configuration average energies of configurations based on single excitation of n=4, 5 and 6 electrons in Sm IX (isoelectronic with W XXI)

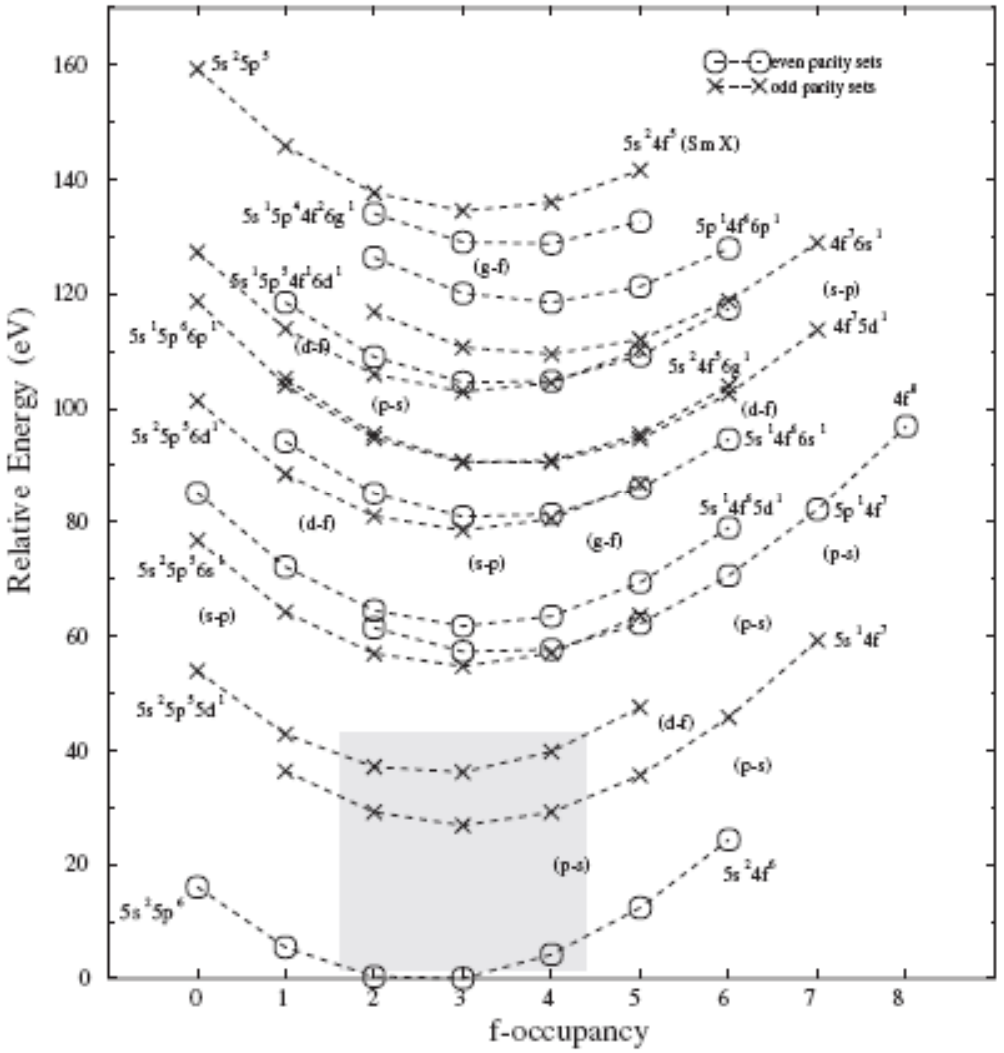

Figure 1. Configuration average energies for a selection of configurations in Xe-like Sm IX. Transitions between the configurations considered in this work are contained within the shaded region.

- Sm IX belongs to the Xe I sequence
- Because of the regrouping of orbitals according to principal quantum number, there is near degeneracy of 4f and 5p binding energies.
- The lowest configuration is $5s^25p^34f^3$
- Configurations of the type $5s^m5p^k4f^n$ (m+k+n= 8) all lie within 60 eV of ground state.
- Level density is enormous (31,086)
- Configuration interaction is very important
- Only 'good quantum numbers are J and π
- Levels and Spectra can only be treated statistically

Energy Level distributions

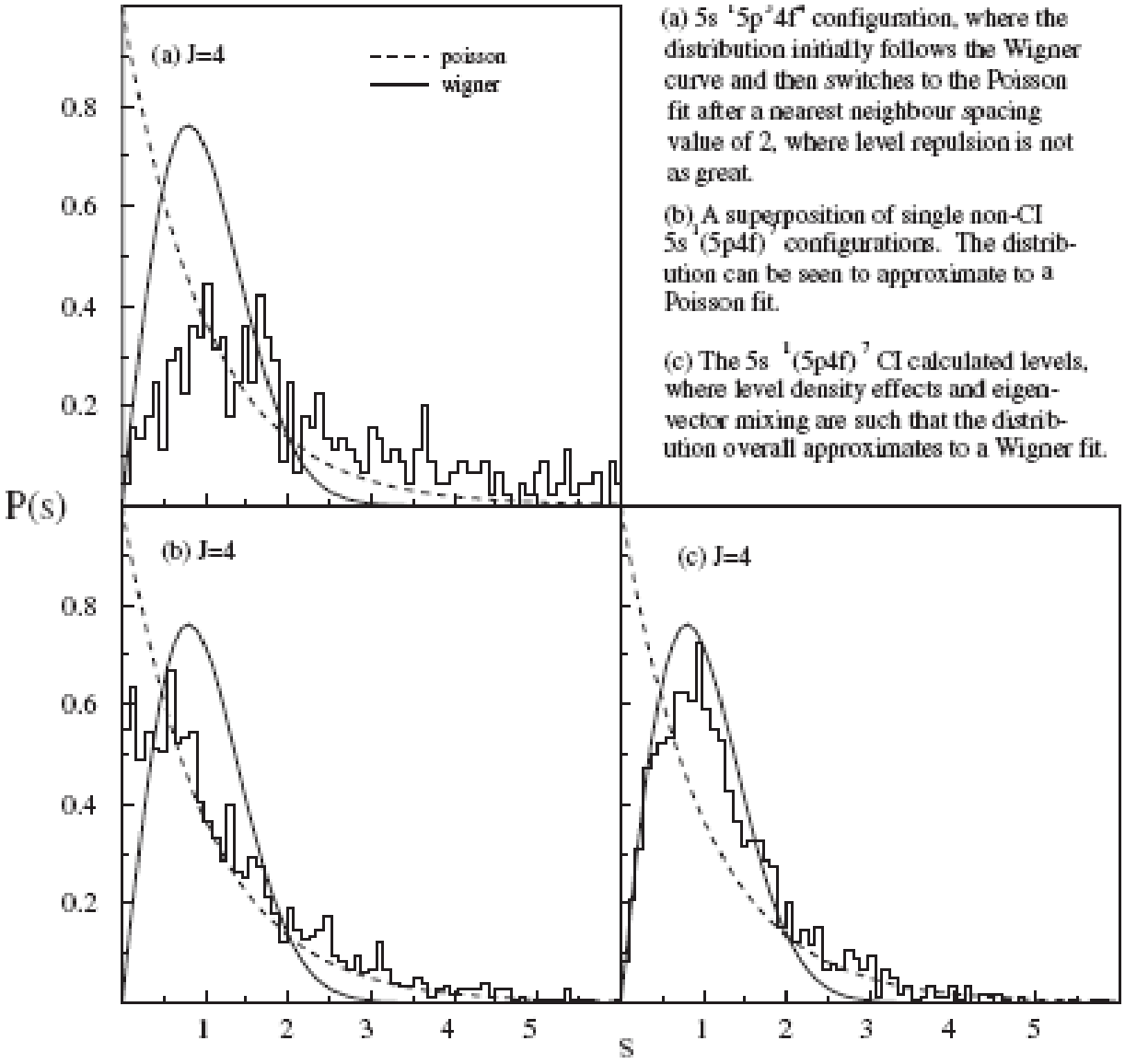

(a) 5s ^{1}5p^{2}4f^7 configuration, where the distribution initially follows the Wigner curve and then switches to the Poisson fit after a nearest neighbour spacing value of 2, where level repulsion is not as great.

(b) A superposition of single non-CI 5s^1(5p4f)^7 configurations. The distribution can be seen to approximate to a Poisson fit.

(c) The 5s ^{1}(5p4f)^7 CI calculated levels, where level density effects and eigenvector mixing are such that the distribution overall approximates to a Wigner fit.

Non CI distribution of nearest neighbour spacings follows a Poisson distribution.

CI leads to a Wigner distribution.

Wigner Distribution:
$P(s)= \pi s/2 \exp(- \pi s^2/4)$

Poisson Distribution:
$P(s)=\exp(-s)$

CI shows Wigner behaviour

Figure 2. Nearest-neighbour distributions for levels of the configurations with CI and non-CI for $J = 4$.

CI increases the number of transitions

- Consider transitions of the type 5p -5d, 4f – 5d and 5s-5p from even $5s^2 5p^{6-n} 4f^n$

- No CI

  $5s^2 5p^6 \leftrightarrow 5s^2 5p^5 5d$

  $5s^2 5p^5 4f \leftrightarrow 5s^2 5p^4 4f 5d$, $5s 5p^6 4f$ and $5s^2 5p^5 4f^0 5d$

  $5s^2 5p^4 4f^2 \leftrightarrow 5s^2 5p^3 4f^2 5d$, $5s 5p^5 4f^2$ and $5s^2 5p^4 4f 5d$

  $5s^2 5p^3 4f^3 \leftrightarrow 5s^2 5p^2 4f^3 5d$, $5s 5p^4 4f^3$ and $5s^2 5p^3 4f^2 5d$

  $5s^2 5p^2 4f^4 \leftrightarrow 5s^2 5p 4f^4 5d$, $5s 5p^3 4f^4$ and $5s^2 5p^2 4f^3 5d$

  $5s^2 5p^1 4f^5 \leftrightarrow 5s^2 5p^0 4f^5 5d$, $5s 5p^2 4f^5$ and $5s^2 5p^3 4f^4 5d$

  $5s^2 4f^6 \leftrightarrow 5s 5p 4f^6$ and $5s^2 4f^5 5d$

- CI:

  $5s^2 5p^6 \leftrightarrow \{5s^2 5p^5 5d, 5s^2 5p^4 4f 5d, 5s 5p^6 4f, 5s^2 5p^5 5d, 5s^2 5p^3 4f^2 5d, 5s 5p^5 4f^2,$
  $5s^2 5p^4 4f 5d, 5s^2 5p^3 4f^2 5d, 5s 5p^5 4f^2, 5s^2 5p^4 4f 5d, 5s^2 5p^2 4f^3 5d, 5s 5p^4 4f^3, 5s^2 5p^3 4f^2 5d,$
  $5s^2 5p 4f^4 5d, 5s 5p^3 4f^4$, $5s^2 5p^2 4f^3 5d$, $5s^2 4f^5 5d$, $5s 5p^2 4f^5$, $5s^2 5p^3 4f^4 5d$, $5s 5p 4f^6$ and
  $5s^2 4f^5 5d\}$

  $5s^2 5p^5 4f \leftrightarrow$ {21 mixed configurations}

  $5s^2 5p^4 4f^2 \leftrightarrow$ {21 mixed configurations}

  $5s^2 5p^3 4f^3 \leftrightarrow$ {21 mixed configurations}

  $5s^2 5p^2 4f^4 \leftrightarrow$ {21 mixed configurations}

  $5s^2 5p^1 4f^5 \leftrightarrow$ {21 mixed configurations}

  $5s^2 4f^6 \leftrightarrow$ {21 mixed configurations}

CI permits all through configuration mixing of both upper and **lower** configurations

Numbers of Lines

No strong lines in observed in W VIII – W XIII. Why?

- Excited configurations can be constructed based on variable numbers of 4f and 5p electrons.
- Form bands of interacting configurations of same J and π.
- Transitions occur between these bands.
- Spectrum is just a continuum with millions of weak lines superimposed on recombination and bremsstrahlung background.

Transition	$L(a-b)$
$(5s^2 5p^5 4f^1) \rightarrow (5s^2 5p^5 4f^0)ng$	82
$(5s^2 5p^4 4f^2) \rightarrow (5s^2 5p^4 4f^1)ng$	24 796
$(5s^2 5p^3 4f^3) \rightarrow (5s^2 5p^3 4f^2)ng$	798 866
$(5s^2 5p^2 4f^4) \rightarrow (5s^2 5p^2 4f^3)ng$	3 997 862
$(5s^2 5p^1 4f^5) \rightarrow (5s^2 5p^1 4f^4)ng$	3 145 502
$(5s^2 5p^0 4f^6) \rightarrow (5s^2 5p^0 4f^5)ng$	253 769
—	—
$(5s^2 5p^5 4f^1) \rightarrow (5s^2 5p^5 4f^0)nd$	91
$(5s^2 5p^4 4f^2) \rightarrow (5s^2 5p^4 4f^1)nd$	19 688
$(5s^2 5p^3 4f^3) \rightarrow (5s^2 5p^3 4f^2)nd$	577 553
$(5s^2 5p^2 4f^4) \rightarrow (5s^2 5p^2 4f^3)nd$	2 774 180
$(5s^2 5p^1 4f^5) \rightarrow (5s^2 5p^1 4f^4)nd$	2 142 405
$(5s^2 5p^0 4f^6) \rightarrow (5s^2 5p^0 4f^5)nd$	171 947
—	—
$(5s^2 5p^6 4f^0) \rightarrow (5s^2 5p^5 4f^0)nd$	3
$(5s^2 5p^5 4f^1) \rightarrow (5s^2 5p^4 4f^1)nd$	1 703
$(5s^2 5p^4 4f^2) \rightarrow (5s^2 5p^3 4f^2)nd$	130 259
$(5s^2 5p^3 4f^3) \rightarrow (5s^2 5p^2 4f^3)nd$	1 491 113
$(5s^2 5p^2 4f^4) \rightarrow (5s^2 5p^1 4f^4)nd$	2 811 276
$(5s^2 5p^1 4f^5) \rightarrow (5s^2 5p^0 4f^5)nd$	691 028
$(5s^2 5p^6 4f^0) \rightarrow (5s^2 5p^5 4f^0)ns$	4
$(5s^2 5p^5 4f^1) \rightarrow (5s^2 5p^4 4f^1)ns$	419
$(5s^2 5p^4 4f^2) \rightarrow (5s^2 5p^3 4f^2)ns$	29 690
$(5s^2 5p^3 4f^3) \rightarrow (5s^2 5p^2 4f^3)ns$	330 682
$(5s^2 5p^2 4f^4) \rightarrow (5s^2 5p^1 4f^4)ns$	615 674
$(5s^2 5p^1 4f^5) \rightarrow (5s^2 5p^0 4f^5)ns$	150 530

Open 4f allows 4d-4f transitions in WVII – W XIII

- Resulting spectrum is just a UTA with millions of weak lines.

Transition	$L(a-b)$
$(5s^2 5p^6 4f^0) \rightarrow (5s^1 5p^6 4f^0)np$	4
$(5s^2 5p^5 4f^1) \rightarrow (5s^1 5p^5 4f^1)np$	971
$(5s^2 5p^4 4f^2) \rightarrow (5s^1 5p^4 4f^2)np$	127 538
$(5s^2 5p^3 4f^3) \rightarrow (5s^1 5p^3 4f^3)np$	2 501 441
$(5s^2 5p^2 4f^4) \rightarrow (5s^1 5p^2 4f^4)np$	8 648 700
$(5s^2 5p^1 4f^5) \rightarrow (5s^1 5p^1 4f^5)np$	5 019 492
$(5s^2 5p^0 4f^6) \rightarrow (5s^1 5p^0 4f^6)np$	310 847
$4d^{10}(5s^2 5p^6 4f^0) \rightarrow 4d^9(5s^2 5p^6 4f^1)$	3
$4d^{10}(5s^2 5p^5 4f^1) \rightarrow 4d^9(5s^2 5p^5 4f^2)$	3 316
$4d^{10}(5s^2 5p^4 4f^2) \rightarrow 4d^9(5s^2 5p^4 4f^3)$	329 120
$4d^{10}(5s^2 5p^3 4f^3) \rightarrow 4d^9(5s^2 5p^3 4f^4)$	4 835 406
$4d^{10}(5s^2 5p^2 4f^4) \rightarrow 4d^9(5s^2 5p^2 4f^5)$	12 773 946
$4d^{10}(5s^2 5p^1 4f^5) \rightarrow 4d^9(5s^2 5p^1 4f^6)$	5 753 400
$4d^{10}(5s^2 5p^0 4f^6) \rightarrow 4d^9(5s^2 5p^0 4f^7)$	279 022
$4d^{10}(5s^2 5p^5 4f^1) \rightarrow 4d^9(5s^2 5p^6 4f^1)$	131
$4d^{10}(5s^2 5p^4 4f^2) \rightarrow 4d^9(5s^2 5p^5 4f^2)$	40 934
$4d^{10}(5s^2 5p^3 4f^3) \rightarrow 4d^9(5s^2 5p^4 4f^3)$	1 491 113
$4d^{10}(5s^2 5p^2 4f^4) \rightarrow 4d^9(5s^2 5p^3 4f^4)$	9 075 627
$4d^{10}(5s^2 5p^1 4f^5) \rightarrow 4d^9(5s^2 5p^2 4f^5)$	9 766 515
$4d^{10}(5s^2 5p^0 4f^6) \rightarrow 4d^9(5s^2 5p^1 4f^6)$	1 431 838

Intensity distribution:

Mean dipole matrix element is zero, and line strengths follow a Porter Thomas distribution (Phys Rev. 104, 483, 1956) distribution: $f(S)=(2\pi S\langle S\rangle)^{1/2}exp(-S/2\langle S\rangle)$, where $S = |\langle m|D|n\rangle|^2$ is the line strength factor

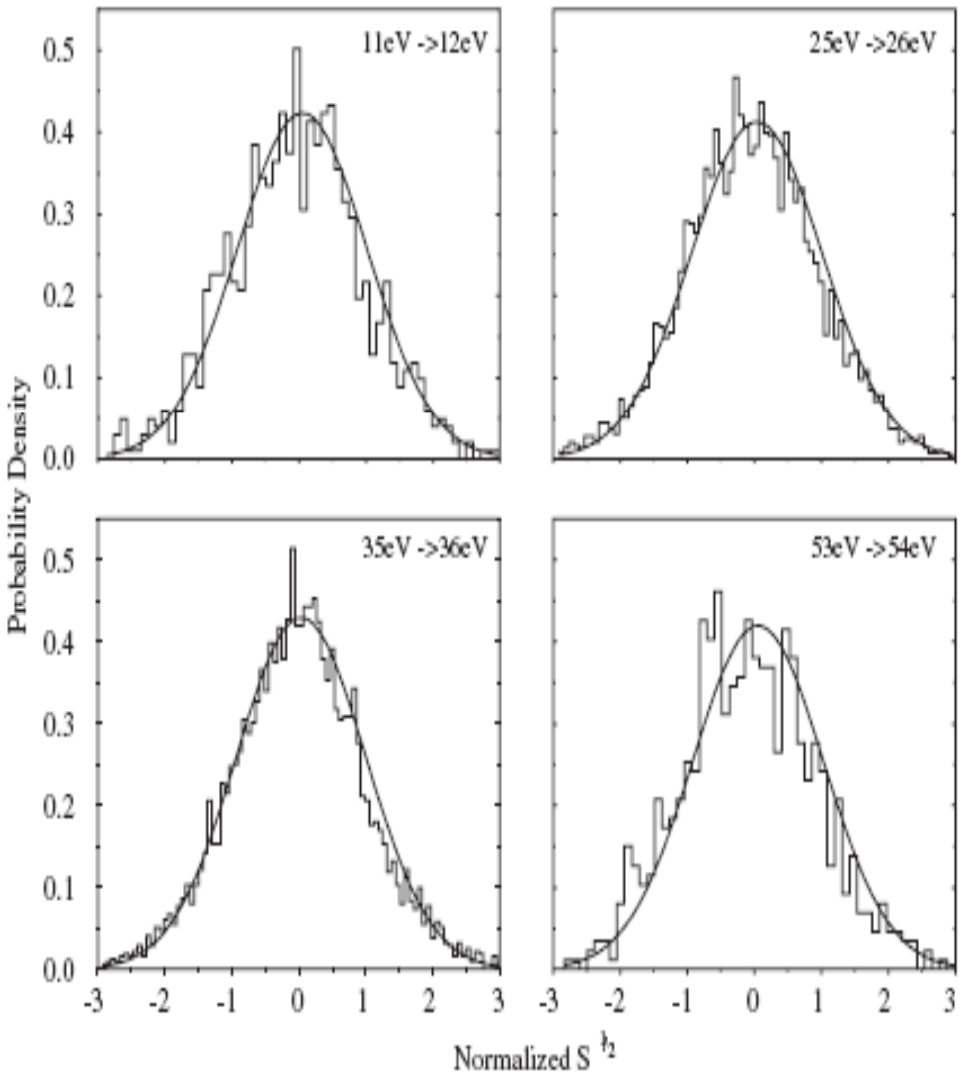

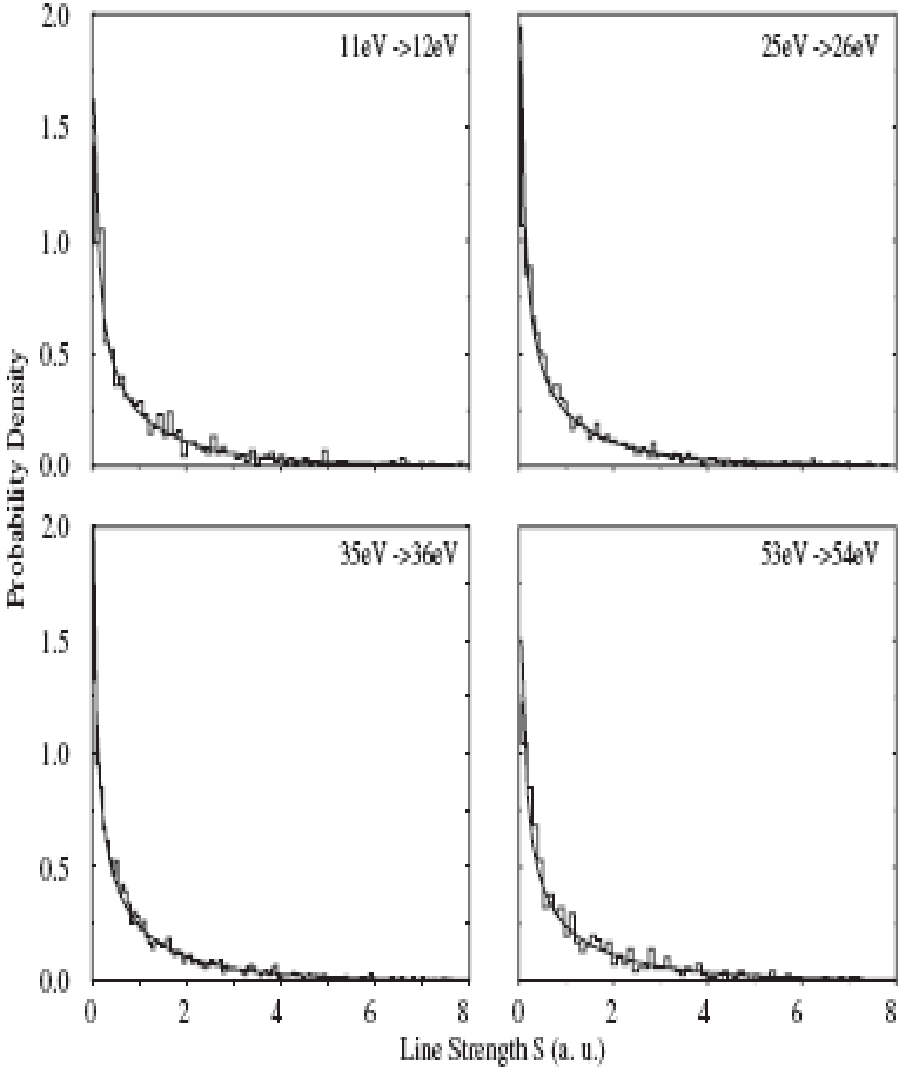

W XIV $4d^{10}5s^{2}4f^{13}$ Ground State

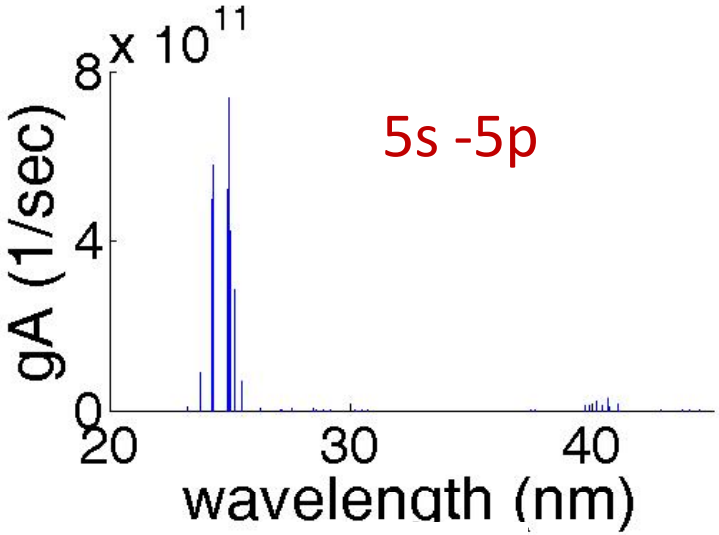

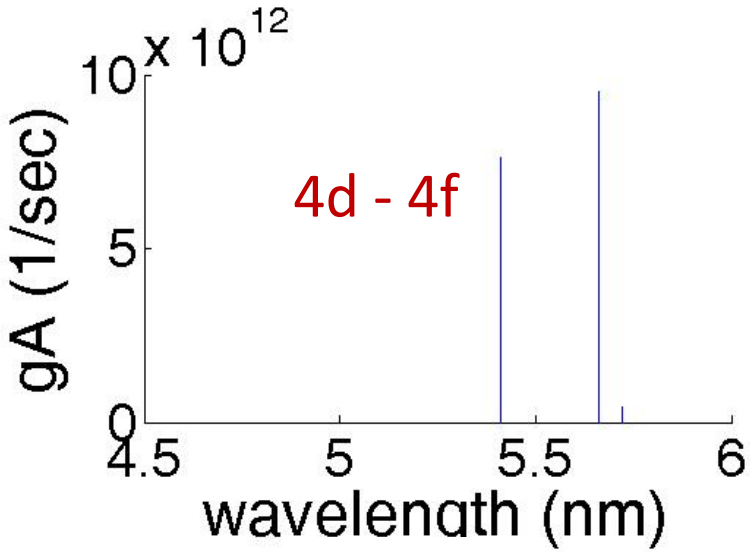

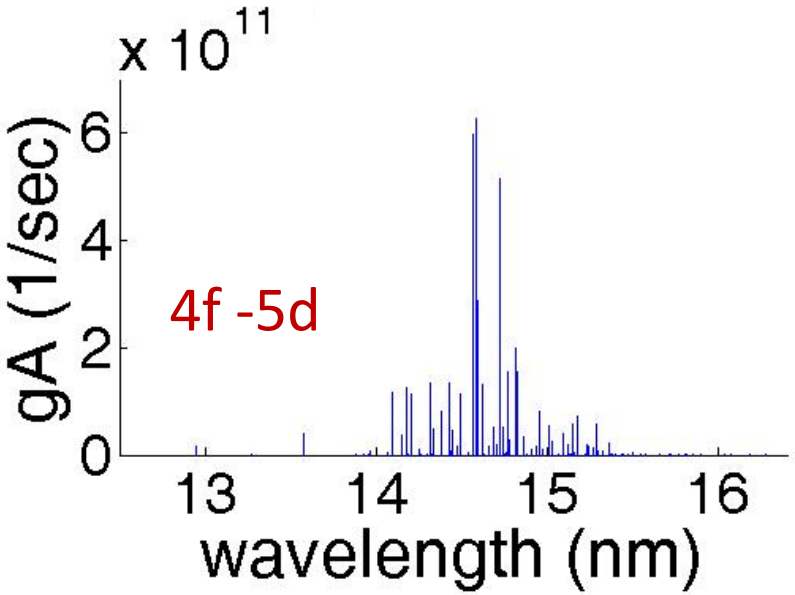

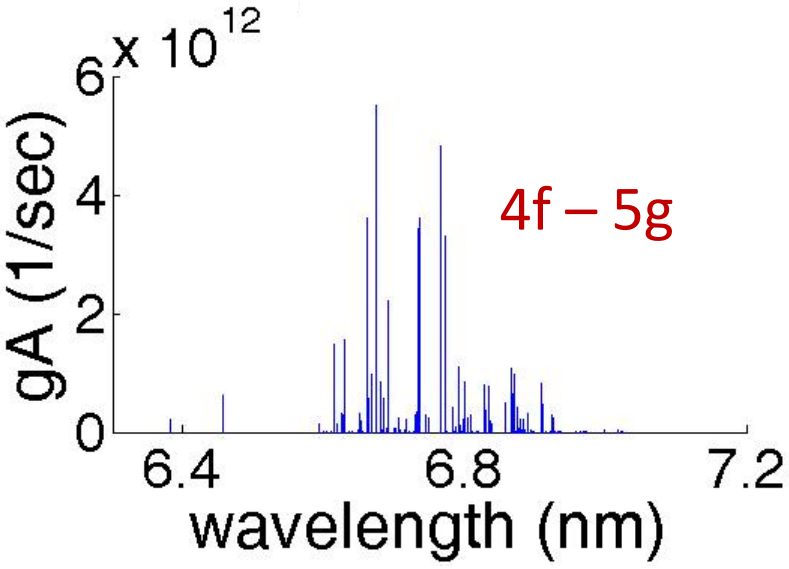

W XIV $4d^{10}4f^{14}5s$ Excited State

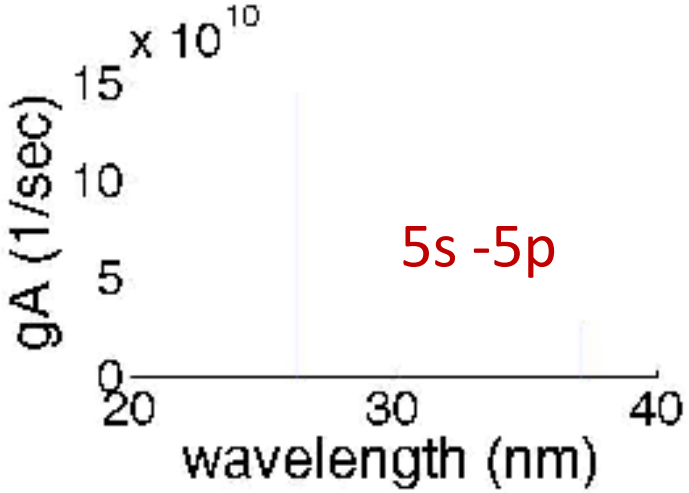

5s -5p

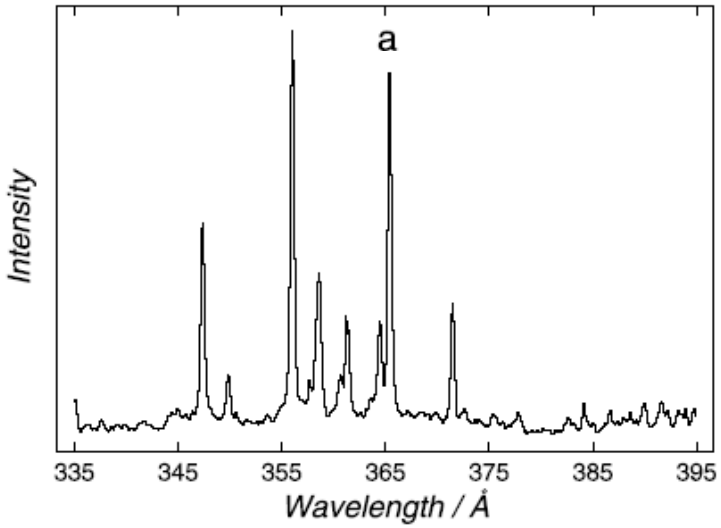

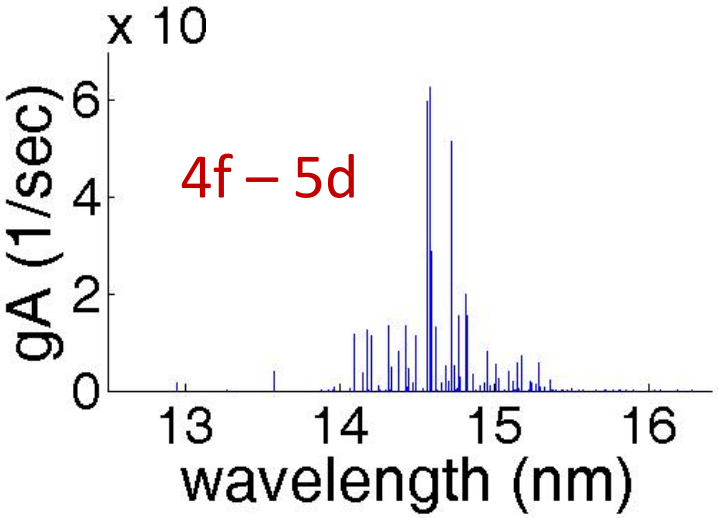

4f – 5d

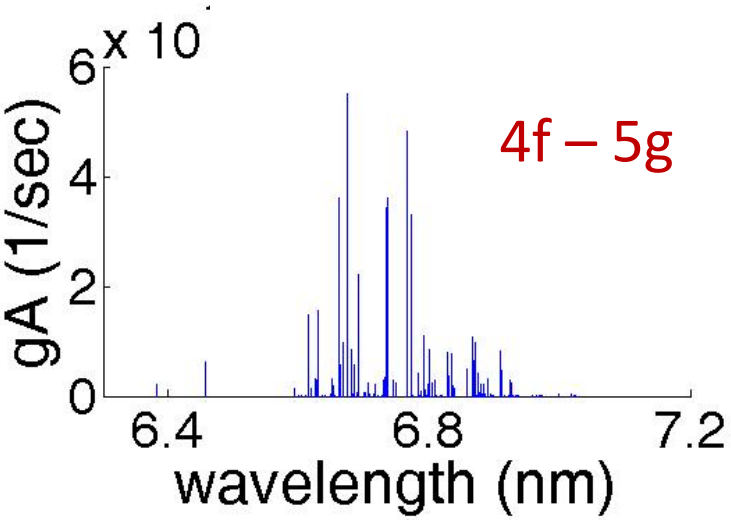

4f – 5g

5s -5p may have been identified in Shanghai EBIT
Hutton et al Nucl. Instrum. Meth. Phys. Res. B 205 (2003) 114.

W XV - XXVIII

W XV: Ground State: $4d^{10}5s^{2}4f^{12}$ but $4d^{10}5s4f^{13}$ and $4d^{10}4f^{14}$ nearby.

W XVI: Ground State : $4d^{10}5s^{2}4f^{11}$ but $4d^{10}5s4f^{12}$ and $4d^{10}4f^{13}$ nearby.

W XVII: Ground State : $4d^{10}5s54f^{11}$ but $4d^{10}4f^{12}$ approx. 2 eV above it. (Kramida and Shirai At. Dat. Nuc. Dat. Tab. **95,** 395, 2009)

W XVIII: Ground State : $4d^{10}4f^{11}$

W XIX - XXVIII: Ground State : $4d^{10}4f^{n}$ $(10\leq n\leq 1)$ 4f subshell strips regularly.

4f – 5g Transitions; W XV - XXVIII

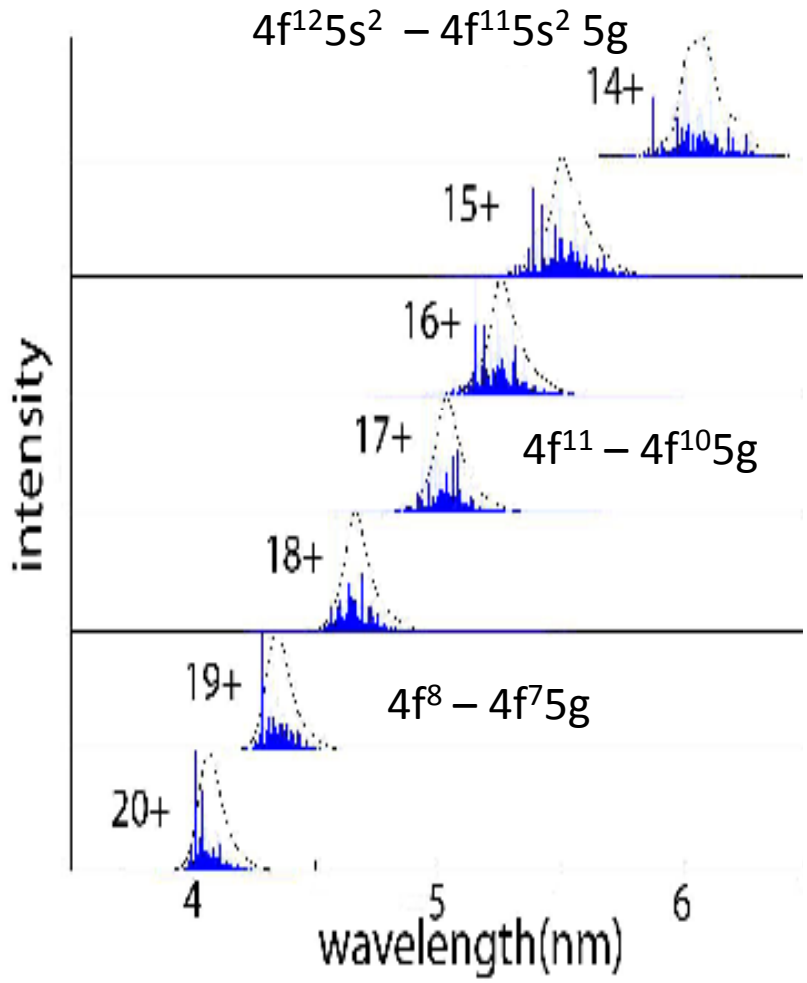

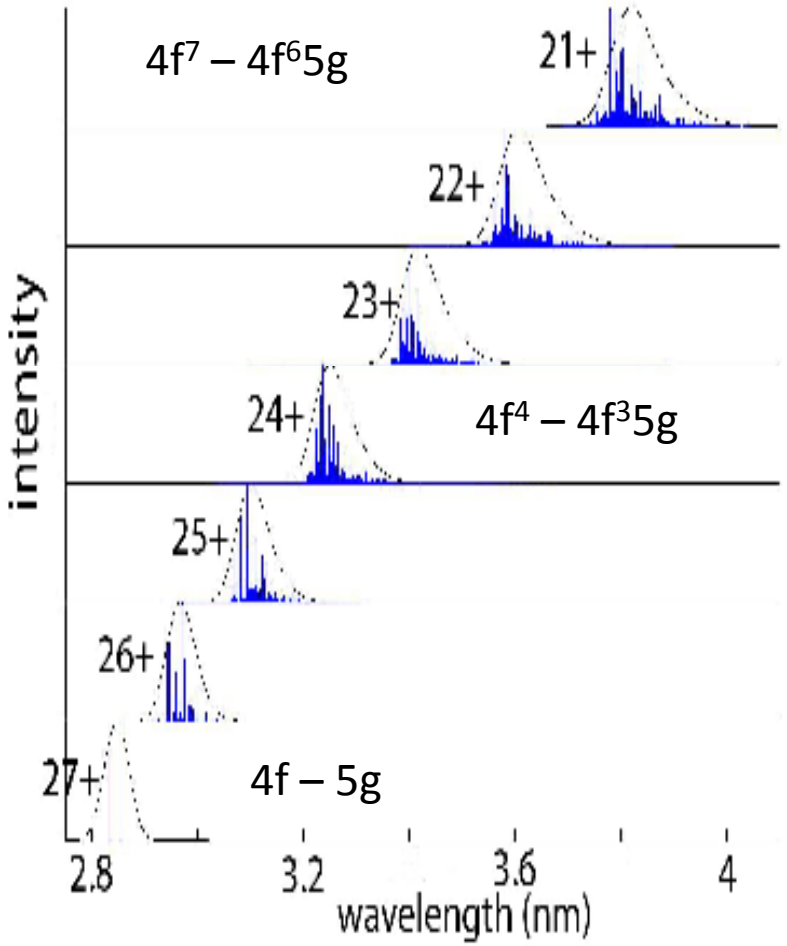

$4f^n$ -$4f^{n-1}5d$ transitions W XV - XXVIII

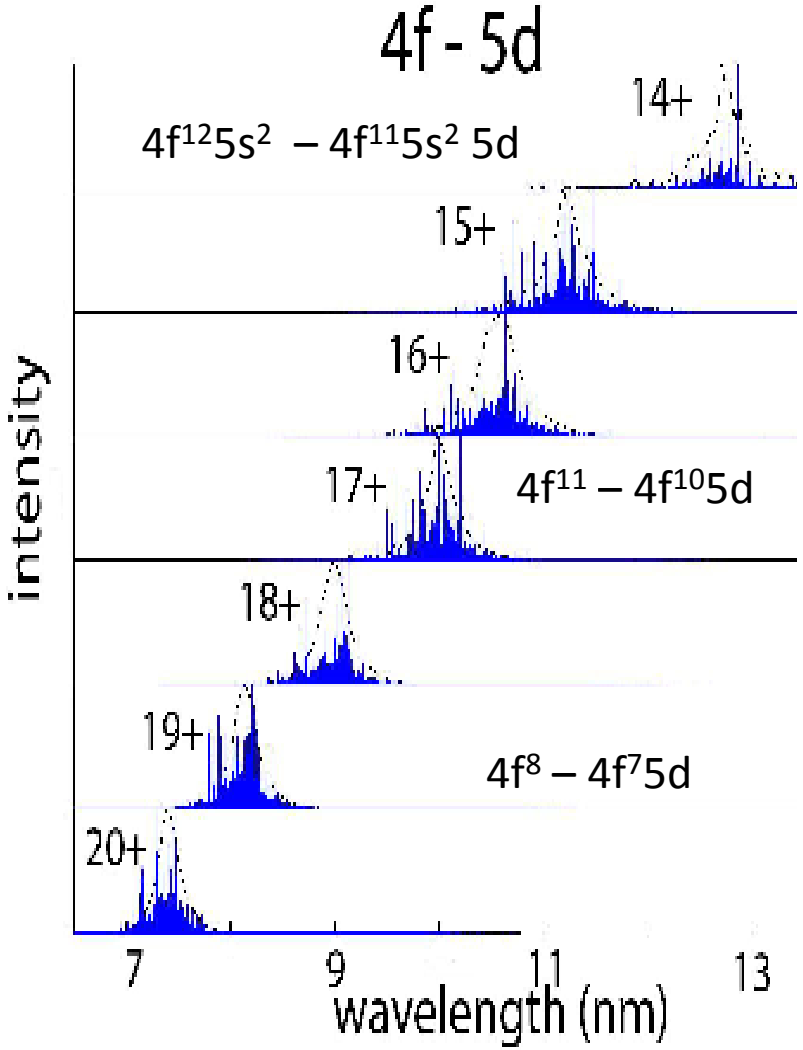

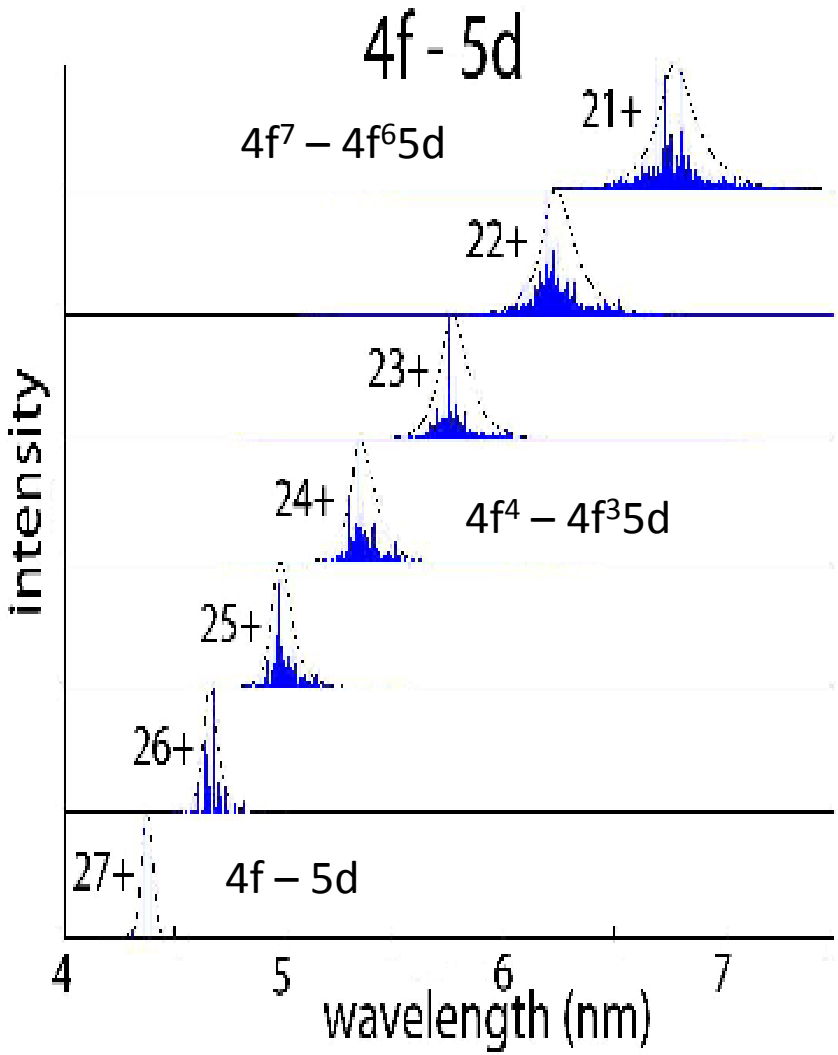

$4d^{10}4f^{11}5s^{m}$– $4d^{9}4f^{12}5s^{m}$ Transitions

$0 \leq m \leq 2$

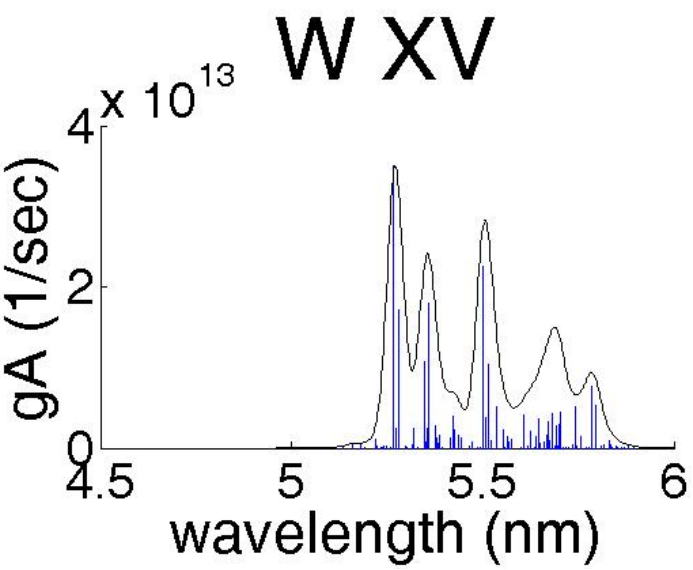

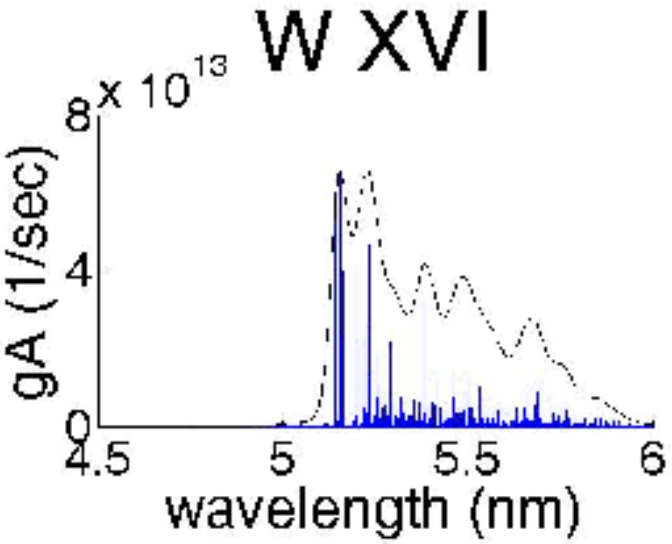

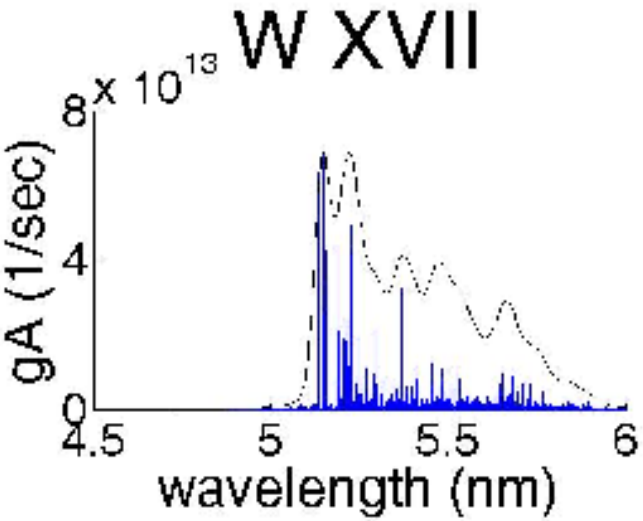

$4d^{10}4f^{n} - 4d^{9}4f^{n+1}$ Transitions $11 \leq n \leq 1$

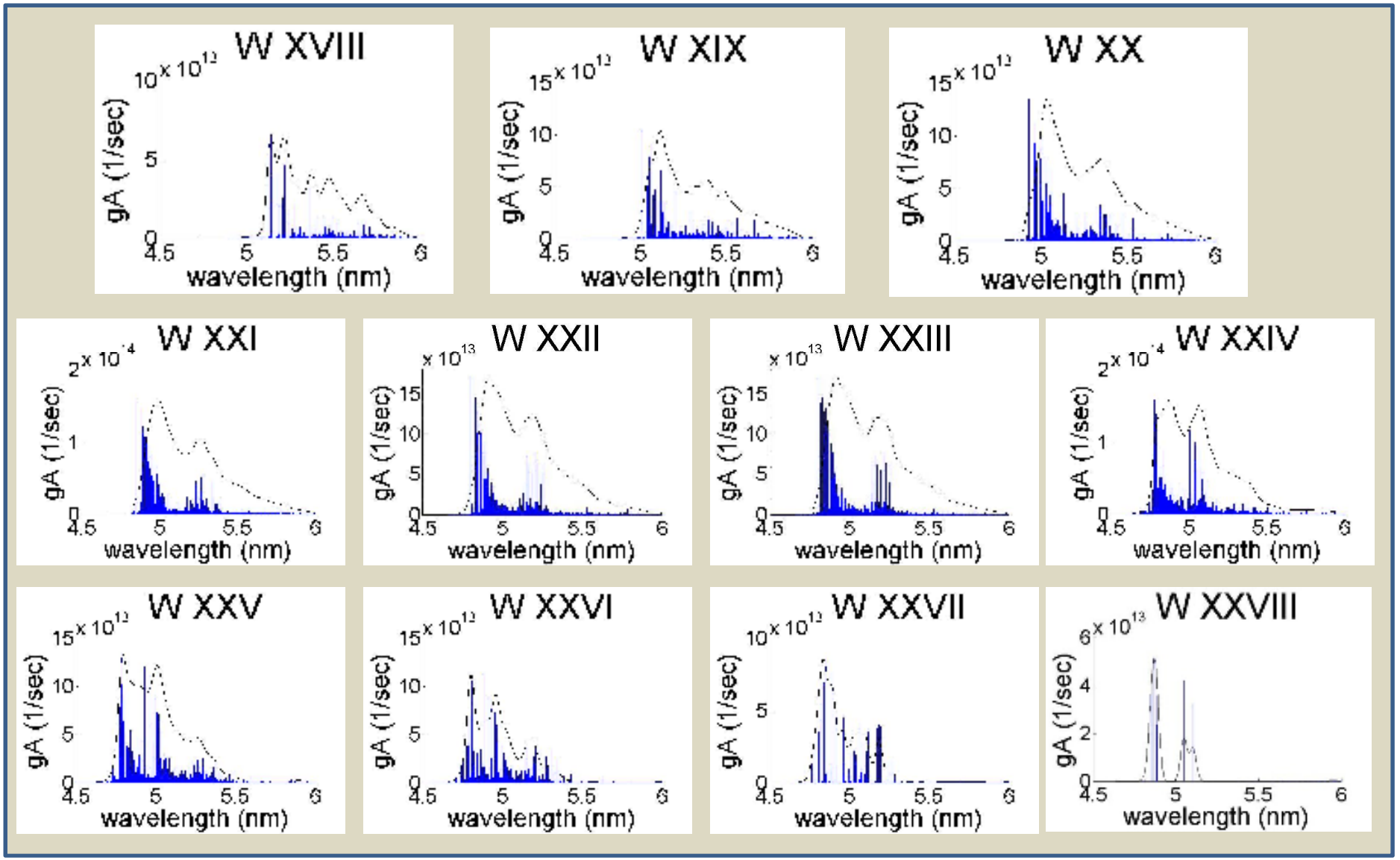

$4p^6 4d^n - 4p^5 4d^{n+1} + 4d^{n-1} 4f$ Transitions $10 \le n \le 1$

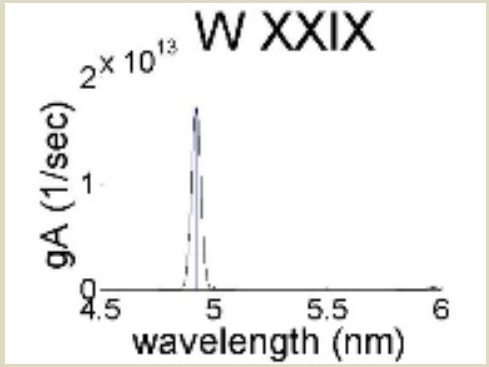

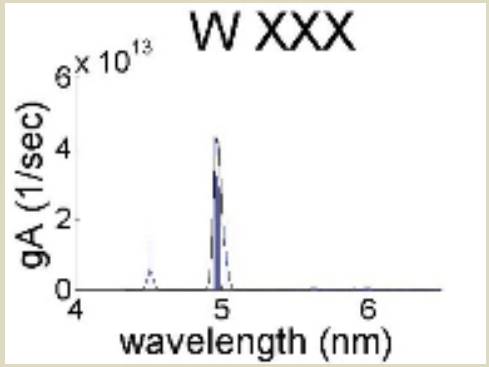

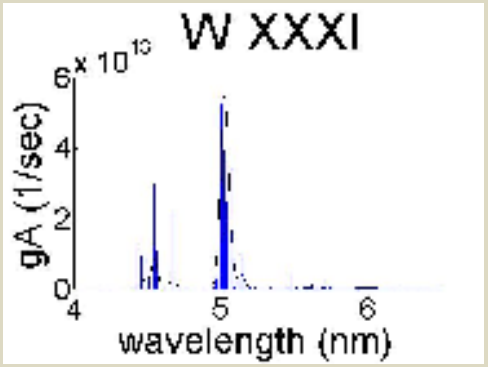

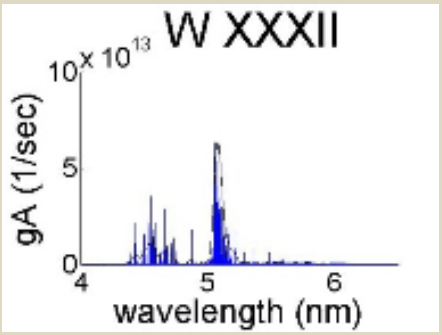

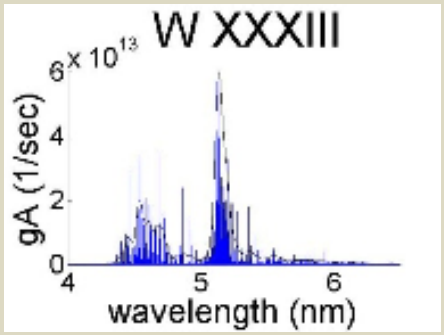

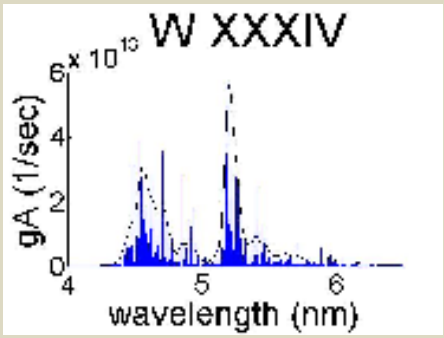

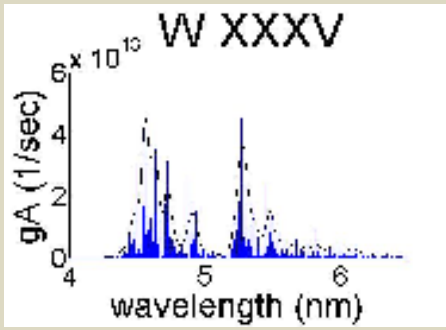

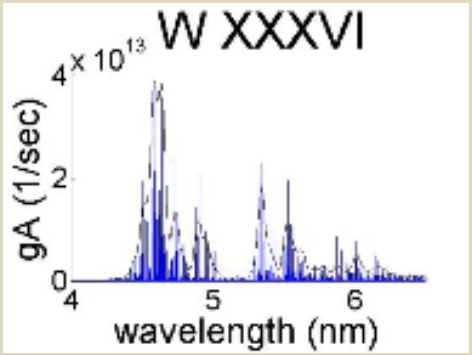

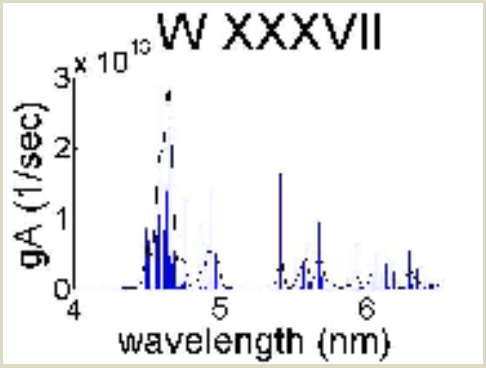

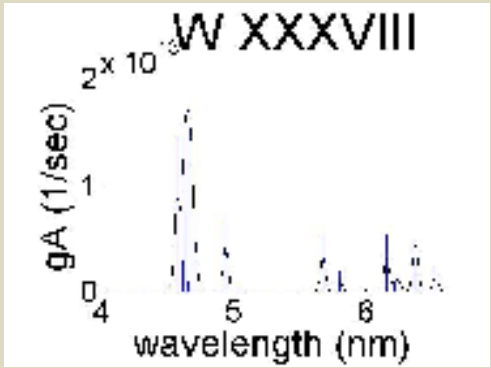

4d – 5p Transitions W XXV- XXXIX

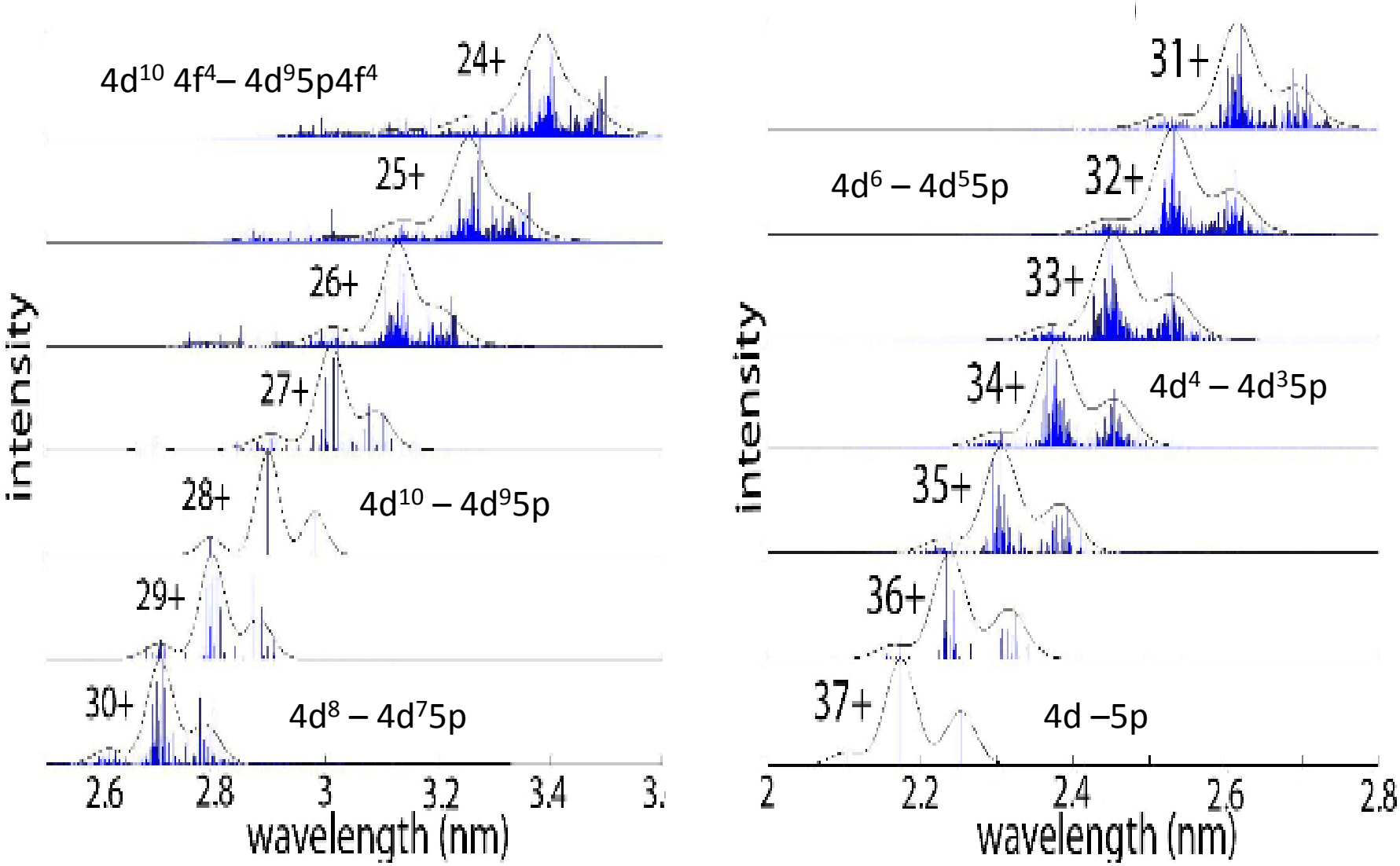

Outline

Background and Previous work

Spectra of W recorded at NIFS

Calculations of Resonance Spectra

- Open 5p subshell spectra and continuum generation
- The special case of W XIV
- Open 4f subshell spectra
- Open 4d subshell spectra
- Open 4p subshell spectra

Effects of low density on spectral complexity

Comparisons and conclusions

Effects of low plasma density

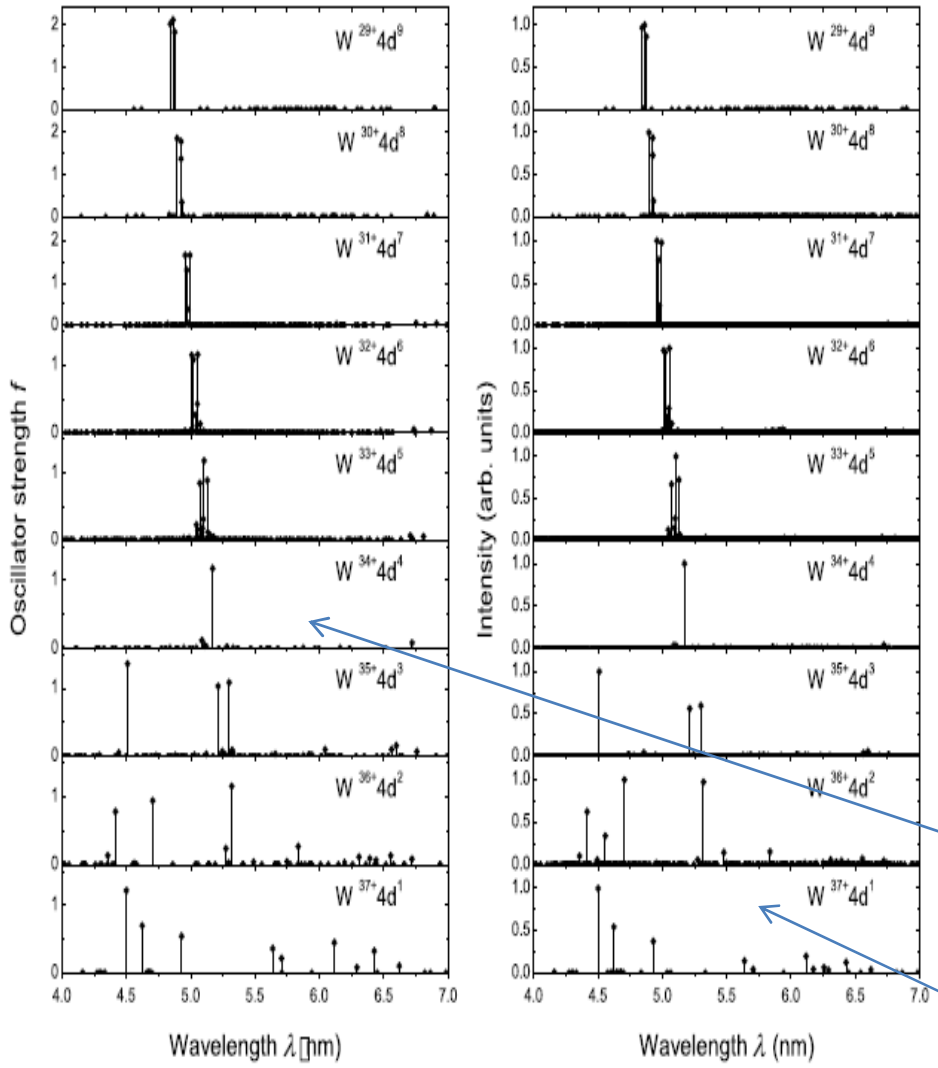

Figure 9. Photoexcitation and emission spectra of W $^{+}$, corresponding to $4p^5 4d\ ^{+1} + 4p^6 4d\ ^{-1} 4f - 4p^6 4d$ transitions, after the photoexcitation from the ground level of the corresponding ion [12]. Calculations are made in the relativistic Dirac–Fock approximation using the code [24].

Jonauskas et al (JPB **40** 2179 2007) and Kucas et al (JPB **42**, 200501 2009) have considered effect of low density.

- Ions mainly in ground state.
- Excitation possible by absorption and collisional excitation.
- Dipole operator dominates collisional process.
- Consider only dipole excitation from ground state.
- Calculate emission from these excited terms.

4d – 4f Transitions excitation of lowest term

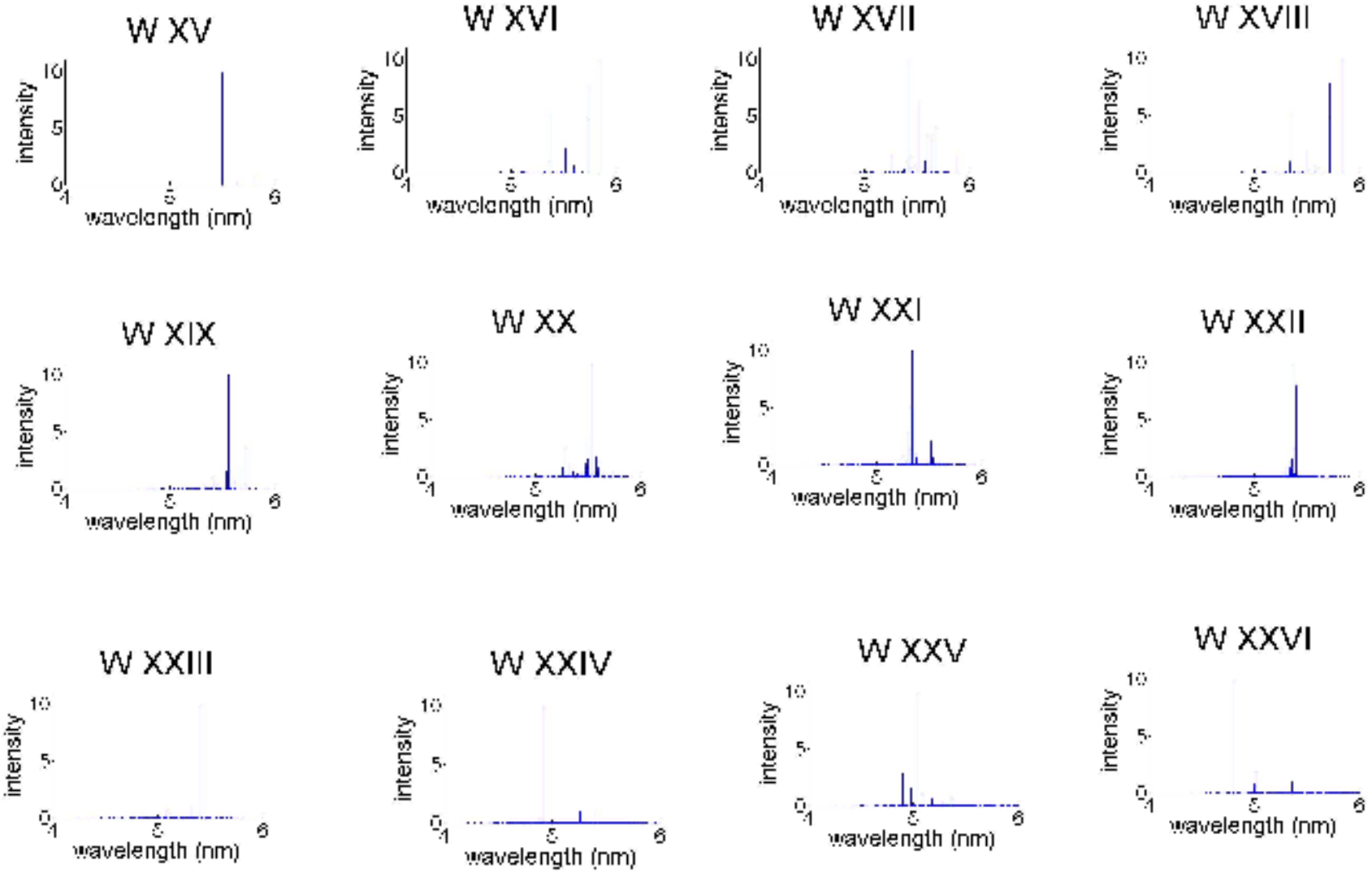

4d – 4f Transitions with excitation of lowest term

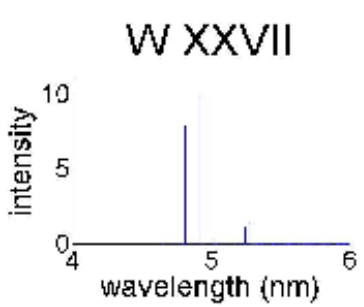

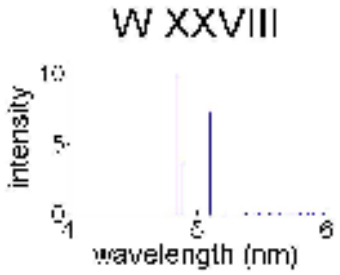

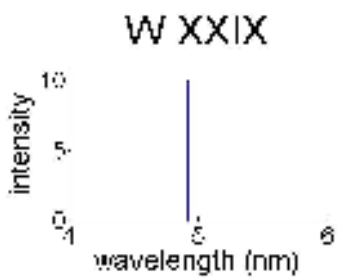

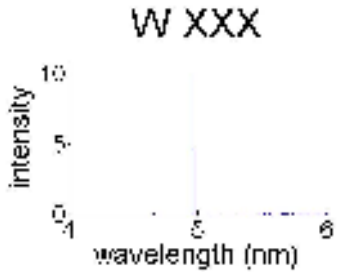

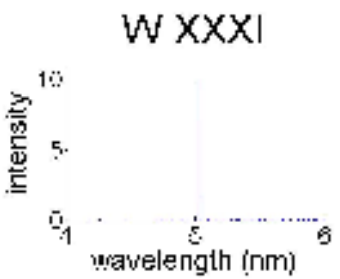

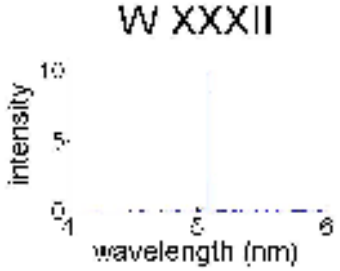

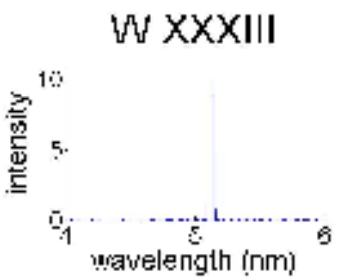

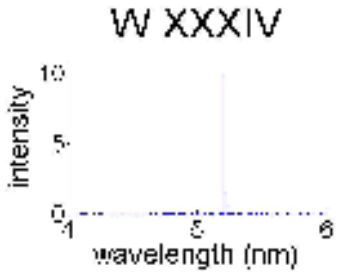

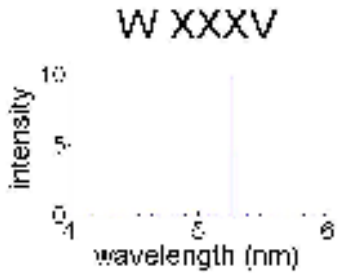

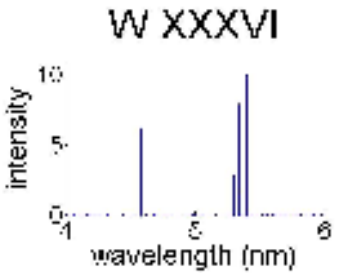

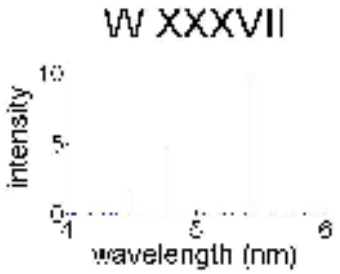

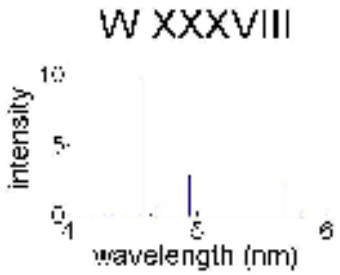

Open 4f subshell Emission

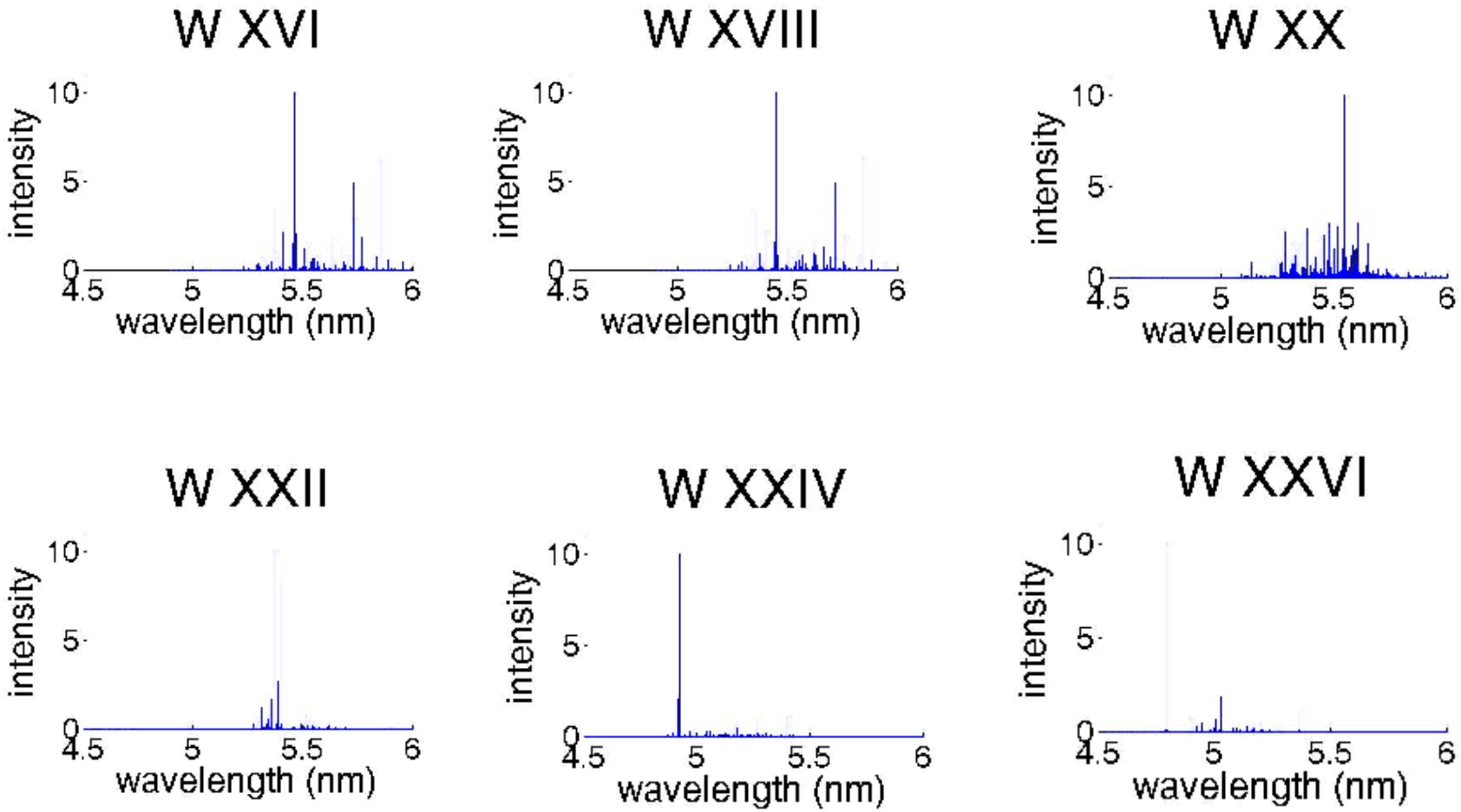

Main Result: Dramatic simplification of the spectrum

Open 4d subshell Emission

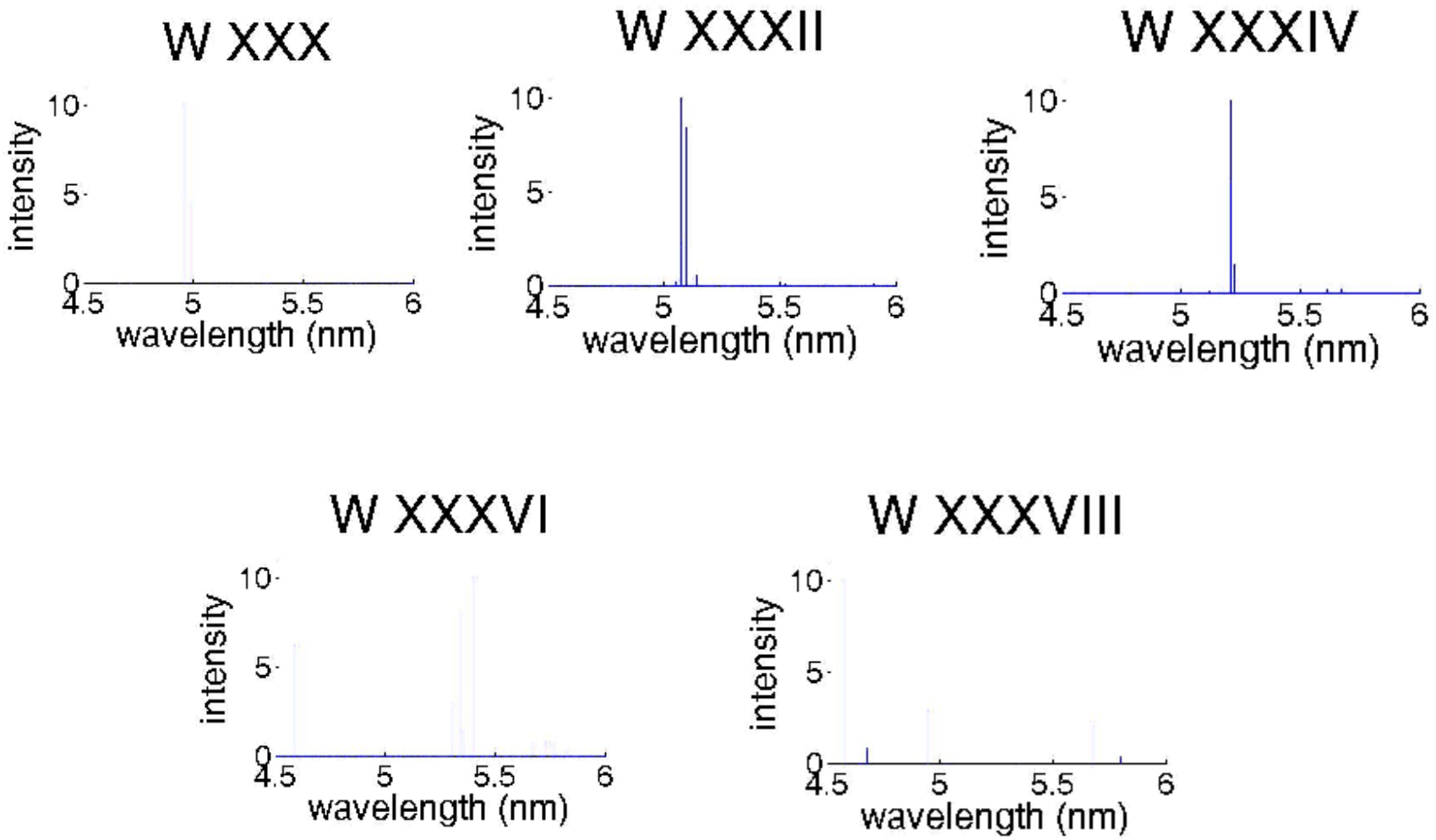

Scatter Plots for n=4 – n =4 Transitions

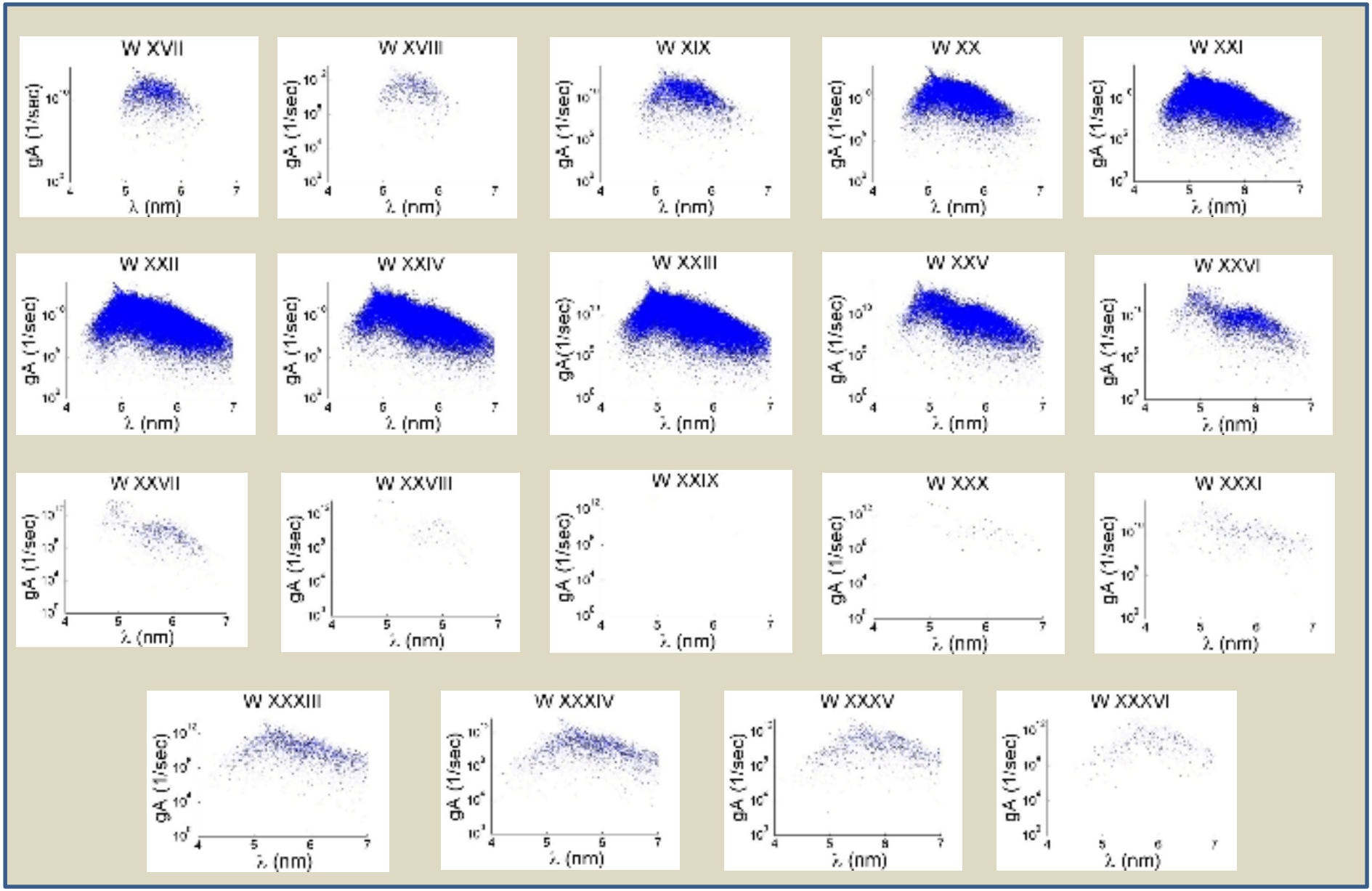

4p-4d Transitions (open 4p subshell ions)

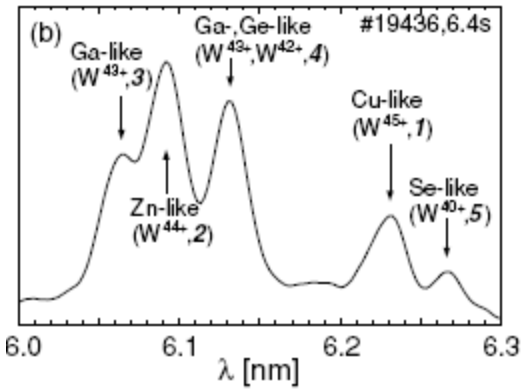

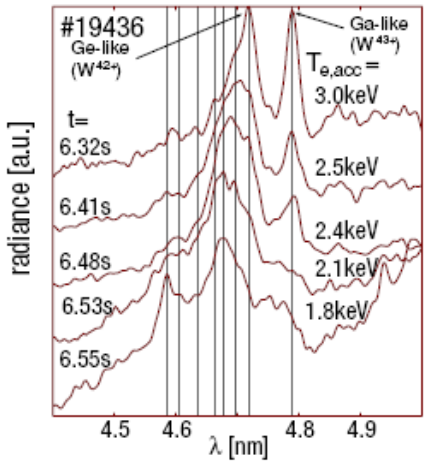

Ion	λ_{expt}	λ^{*}_{expt}	λ_{th}	I_{CR}	Lower level	J_L	Upper level	J_U
	47.16 b	46.9 b	46.69	4.9	$4s^2\,4p_{1/2}^2\,4p_{3/2}$	3/2	73% $4s^2(4p_{1/2}\,4p_{3/2})_2\,4d_{3/2}$	3/2
	47.16 b	46.9 b	46.64	2.0	$4s^2\,4p_{1/2}^2\,4p_{3/2}$	3/2	88% $4s^2(4p_{1/2}\,4p_{3/2})_2\,4d_{3/2}$	1/2
	47.16 b	46.9 b	47.07	5.7	$4s^2\,4p_{1/2}^2\,4p_{3/2}$	3/2	39% $4s^2(4p_{1/2}\,4p_{3/2})_1\,4d_{3/2}$	5/2
	60.71	60.6	60.26	2.9	$4s^2\,4p_{1/2}^2\,4p_{3/2}$	3/2	85% $4s\,4p_{1/2}^2(4p_{3/2}^2)_2$	3/2
	64.82	64.9	64.69	3.1	$4s^2\,4p_{1/2}^2\,4p_{3/2}$	3/2	61% $4s\,4p_{1/2}^2(4p_{3/2}^2)_2$	5/2
	70.15		69.96	1.5	$4s^2\,4p_{1/2}^2\,4p_{3/2}$	3/2	63% $4s^2\,4p_{1/2}^2\,4d_{5/2}$	5/2
	46.88 b	46.9 b	46.30	1.6	$4s^2\,4p_{1/2}^2\,4p_{3/2}^2$	0	78% $(4s^2\,4p_{1/2}(4p_{3/2}^2)_0)_{1/2}\,4d_{3/2}$	1
	46.88 b	46.9 b	46.09	2.6	$4s^2\,4p_{1/2}^2\,4p_{3/2}^2$	2	75% $(4s^2\,4p_{1/2}(4p_{3/2}^2)_2)_{5/2}\,4d_{3/2}$	1
	46.88 b	46.9 b	46.30	3.6	$4s^2\,4p_{1/2}^2\,4p_{3/2}^2$	2	67% $(4s^2\,4p_{1/2}(4p_{3/2}^2)_2)_{5/2}\,4d_{3/2}$	2
	46.88 b	46.9 b	46.34	4.8	$4s^2\,4p_{1/2}^2\,4p_{3/2}^2$	2	50% $(4s^2\,4p_{1/2}(4p_{3/2}^2)_2)_{3/2}\,4d_{3/2}$	3
	62.60		62.34	2.7	$4s^2\,4p_{1/2}^2\,4p_{3/2}^2$	2	69% $4s\,4p_{1/2}^2\,4p_{3/2}^3$	2
	65.81 b	65.8 b	64.79	4.9	$4s^2\,4p_{1/2}^2\,4p_{3/2}^2$	2	89% $4s^2\,4p_{1/2}^2\,4p_{3/2}\,4d_{5/2}$	3
	46.81 b	46.9 b	46.46	4.8	$4s^2\,4p_{1/2}^2\,4p_{3/2}^3$	3/2	77% $4s^2(4p_{1/2}\,4p_{3/2}^3)_2\,4d_{3/2}$	1/2
	46.81 b	46.9 b	46.63	4.9	$4s^2\,4p_{1/2}^2\,4p_{3/2}^3$	3/2	41% $4s^2(4p_{1/2}\,4p_{3/2}^3)_2\,4d_{3/2}$	3/2
	46.81 b	46.9 b	46.64	9.4	$4s^2\,4p_{1/2}^2\,4p_{3/2}^3$	3/2	47% $4s^2(4p_{1/2}\,4p_{3/2}^3)_2\,4d_{3/2}$	5/2
	64.74	64.6	64.69	11.0	$4s^2\,4p_{1/2}^2\,4p_{3/2}^3$	3/2	70% $4s^2(4p_{1/2}^2\,4p_{3/2}^3)_2\,4d_{5/2}$	5/2
	65.76 b	65.8 b	65.69	5.9	$4s^2\,4p_{1/2}^2\,4p_{3/2}^3$	3/2	66% $4s^2(4p_{1/2}^2\,4p_{3/2}^3)_2\,4d_{5/2}$	3/2
	46.40 b		46.06	26.0	$4s^2\,4p^6$	0	92% $4s^2\,4p_{1/2}^5\,4d_{3/2}$	1
	63.98		63.25	24.0	$4s^2\,4p^6$	0	85% $4s^2\,4p_{3/2}^5\,4d_{5/2}$	1
	49.52		49.06	8.8	$4s^2\,4p^6\,4d_{3/2}$	3/2	82% $4s^2\,4p_{1/2}^5(4d_{3/2}^2)_2$	5/2
	56.86		56.04	4.8	$4s^2\,4p^6\,4d_{3/2}$	3/2	53% $4s^2\,4p^6\,4f_{5/2}$	5/2
	57.74		56.72	1.8	$4s^2\,4p^6\,4d_{3/2}$	3/2	40% $4s^2\,4p_{3/2}^5(4d_{5/2}^2)_4$	5/2
	64.82		63.87	5.3	$4s^2\,4p^6\,4d_{3/2}$	3/2	59% $4s^2(4p_{3/2}^5\,4d_{3/2})_3\,4d_{5/2}$	3/2
Sr-like W^{36+}	54.14		53.21	16.1	$4s^2\,4p^6\,4d_{3/2}^2$	2	69% $4s^2\,4p^6\,4d_{3/2}\,4f_{5/2}$	3

4p-4d gives two groups of lines near 4.7 and 6.5 nm Radke *et al* PRA64,012520, 2001

4p-4d Transitions (open 4p subshell ions)

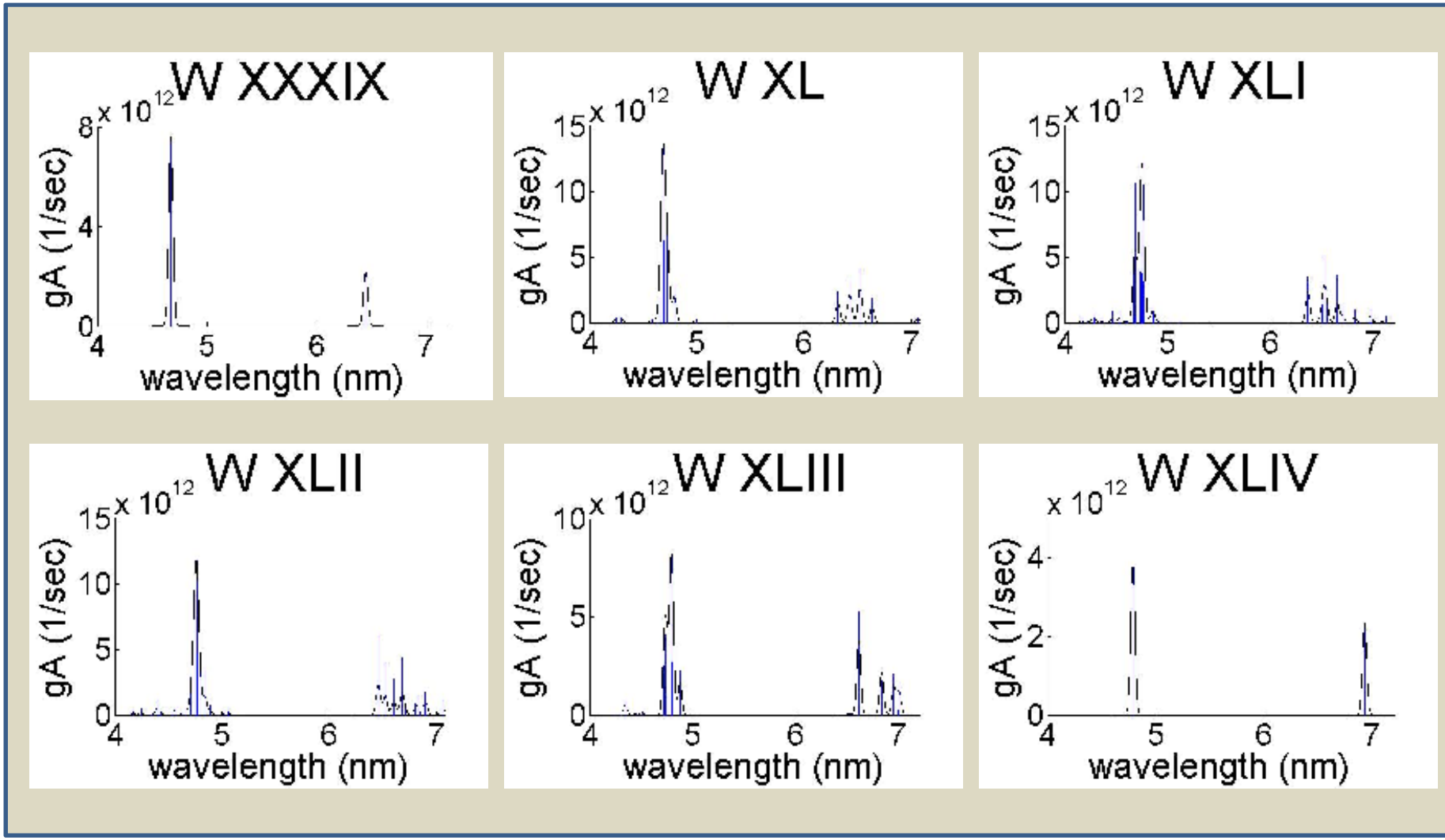

Outline

Background and Previous work

Spectra of W recorded at NIFS

Calculations of Resonance Spectra

- Open 5p subshell spectra and continuum generation
- The special case of W XIV
- Open 4f subshell spectra
- Open 4d subshell spectra
- Open 4p subshell spectra

Effects of low density on spectral complexity

Comparisons and conclusions

UTA Approach

Cowan data was used to generate UTA statistics for each family of transitions

Ion	Transition	No. of Lines	Σ gf	Mean λ (nm)	σ (nm)	Skewness	Kurtosis
W XV	$4d^{10}4f^{12}5s^2$ - $4d^{9}4f^{13}5s^2$	108	104.80	5.49	0.18	0.27	1.86
W XVI	$4d^{10}4f^{11}5s^2$ - $4d^{9}4f^{12}5s^2$	1727	620.09	5.42	0.21	0.46	2.24
W XVII	$4d^{10}4f^{11}5s$ - $4d^{9}4f^{12}5s$	6712	1233.96	5.41	0.21	0.46	2.24
W XVIII	$4d^{10}4f^{11}$ - $4d^{9}4f^{12}$	1728	612.72	5.40	0.21	0.46	2.24
W XIX	$4d^{10}4f^{10}$ - $4d^{9}4f^{11}$	14084	2211.41	5.34	0.23	0.59	2.55
W XX	$4d^{10}4f^{9}$ - $4d^{9}4f^{10}$	64003	5447.60	5.28	0.24	0.70	2.87
W XXI	$4d^{10}4f^{8}$ - $4d^{9}4f^{9}$	171124	9636.79	5.22	0.25	0.81	3.21
W XXII	$4d^{10}4f^{7}$ - $4d^{9}4f^{8}$	277823	12629.39	5.17	0.25	0.93	3.64
W XXIII	$4d^{10}4f^{6}$ - $4d^{9}4f^{7}$	277823	12393.93	5.13	0.25	1.07	4.20
W XXIV	$4d^{10}4f^{5}$ - $4d^{9}4f^{6}$	171128	9111.54	5.09	0.25	1.24	4.98
W XV	$4d^{10}4f^{4}$ - $4d^{9}4f^{5}$	64004	4960.45	5.05	0.24	1.48	6.16
W XVI	$4d^{10}4f^{3}$ - $4d^{9}4f^{4}$	14086	1941.48	5.02	0.22	1.84	8.14
W XVII	$4d^{10}4f^{2}$ - $4d^{9}4f^{3}$	1728	518.12	4.99	0.20	2.45	11.95
W XVIII	$4d^{10}4f$ - $4d^{9}4f^{2}$	108	84.39	4.96	0.17	3.71	21.46
W XIX	$4d^{10}$ - $4d^{9}4f$	3	6.38	4.91	0.12	9.04	83.02
W XX	$4p^{6}4d^{9}$ – $4p^{5}4d^{10}$+$4p^{6}4d^{8}4f$	84	60.24	4.95	0.22	4.45	38.24
W XXI	$4p^{6}4d^{8}$ – $4p^{5}4d^{9}$+$4p^{6}4d^{7}4f$	781	256.22	4.99	0.29	3.05	21.44
W XXII	$4p^{6}4d^{7}$– $4p^{5}4d^{8}$+$4p^{6}4d^{6}4f$	3291	646.90	5.03	0.36	2.29	13.73
W XXIII	$4p^{6}4d^{6}$ – $4p^{5}4d^{7}$+$4p^{6}4d^{5}4f$	7188	1073.97	5.08	0.42	1.80	9.43
W XXXIV	$4p^{6}4d^{5}$ – $4p^{5}4d^{6}$+$4p^{6}4d^{4}4f$	8715	1224.78	5.12	0.48	1.45	6.75

UTA Results

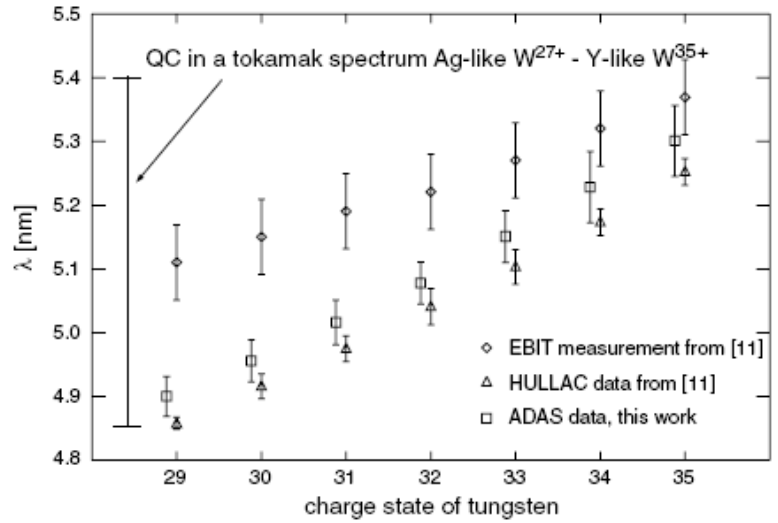
QC in a tokamak spectrum Ag-like W27+ - Y-like W35+
λ [nm]
charge state of tungsten
EBIT measurement from [11]
HULLAC data from [11]
ADAS data, this work

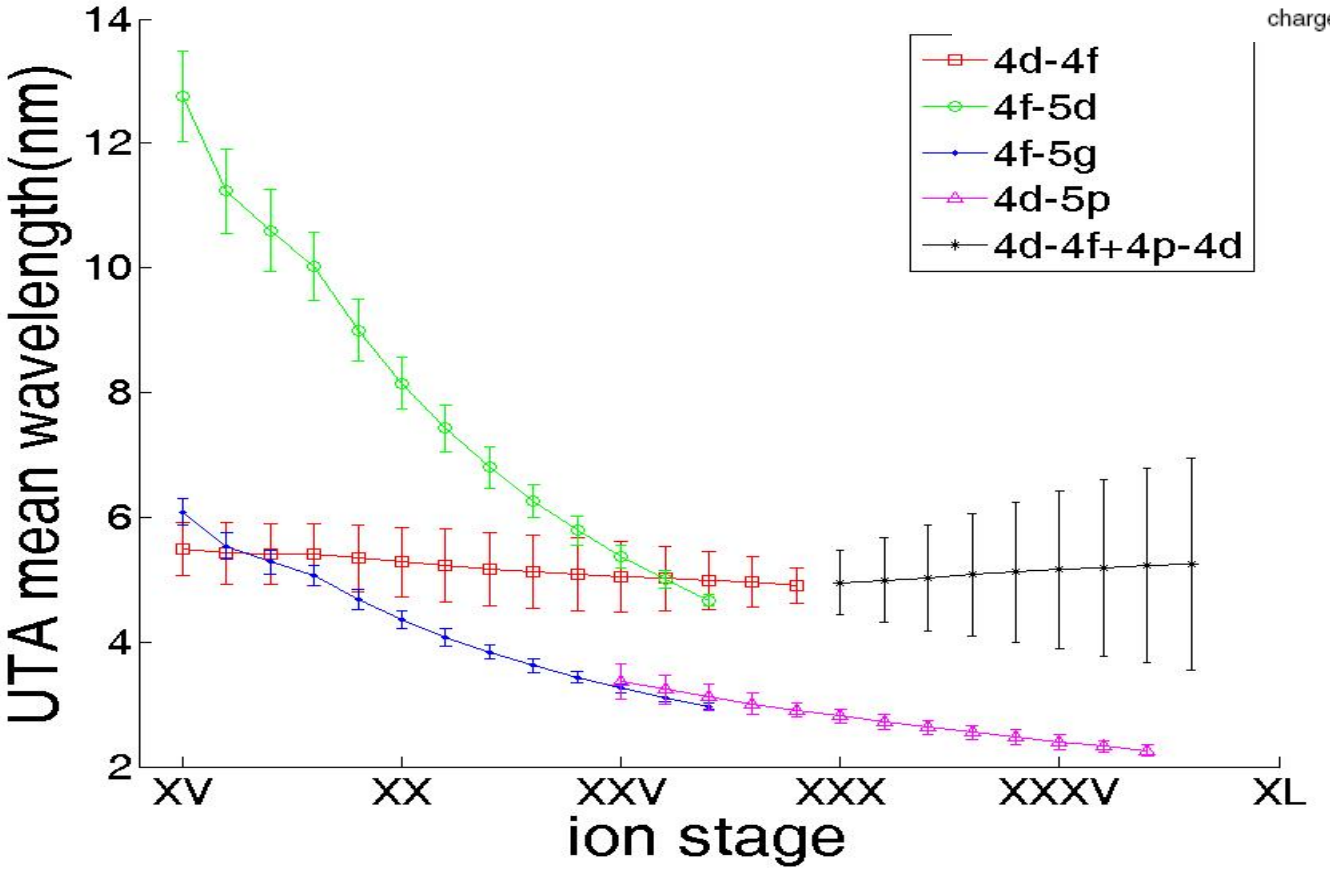
4d-4f
4f-5d
4f-5g
4d-5p
4d-4f+4p-4d
UTA mean wavelength(nm)
ion stage
XV
XX
XXV
XXX
XXXV
XL

Comparisons with other work

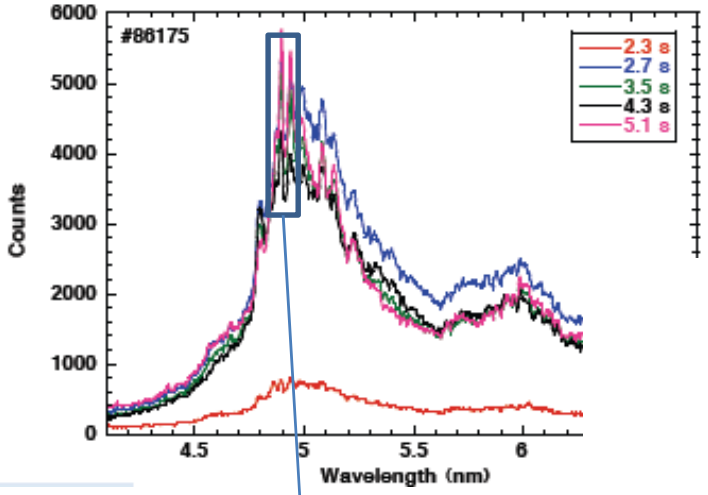

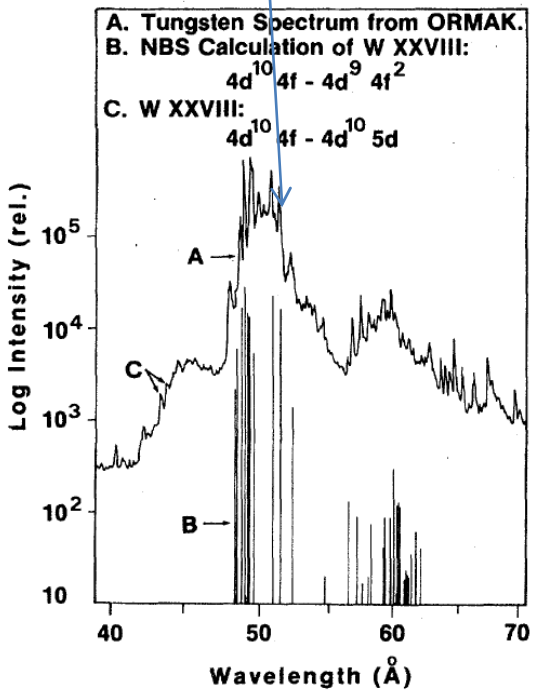

Sugar, Kaufman & Rowan, JOSA B10, 1977 (1993) W XXVIII, XIX and XX

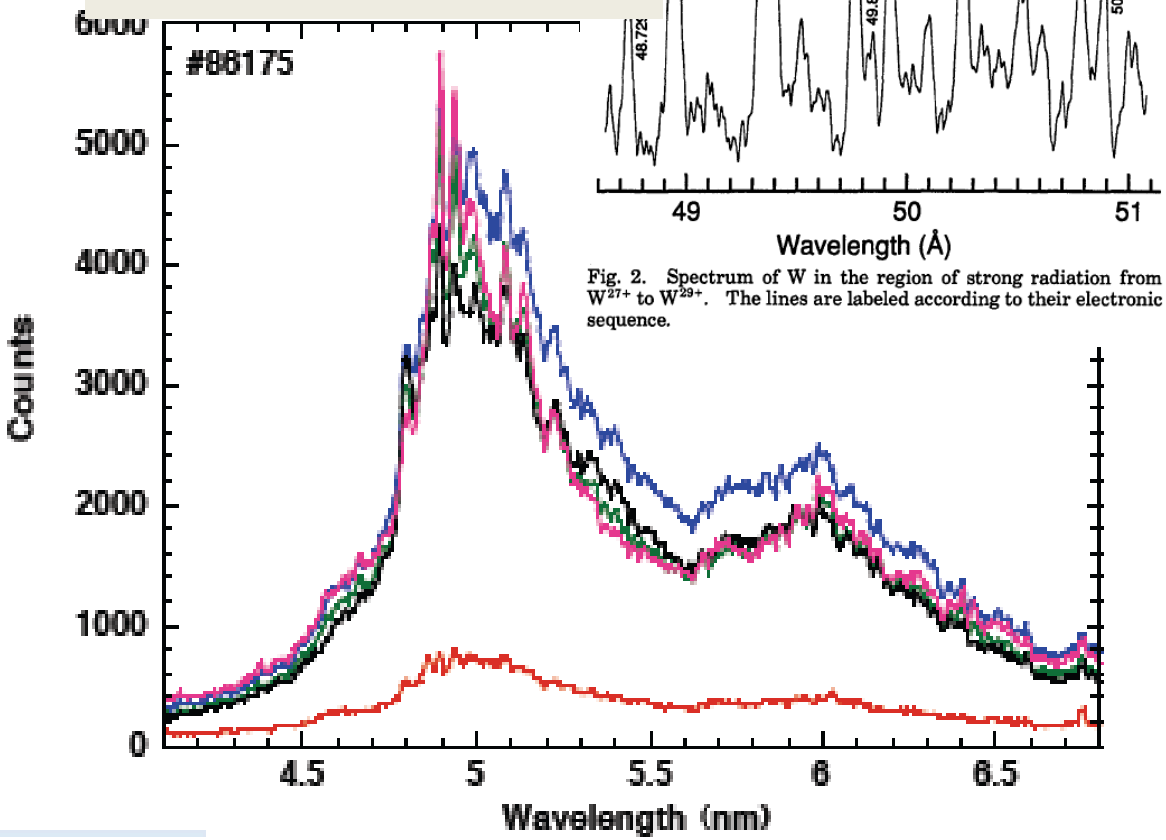

Fig. 2. Spectrum of W in the region of strong radiation from W^{27+} to W^{29+}. The lines are labeled according to their electronic sequence.

Tentative Conclusions

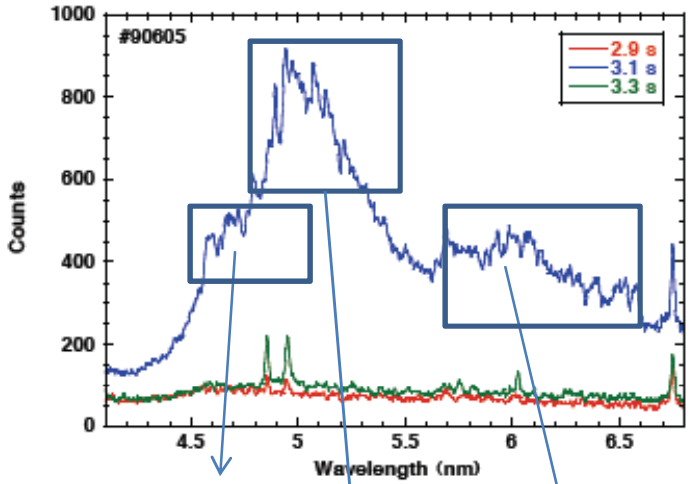

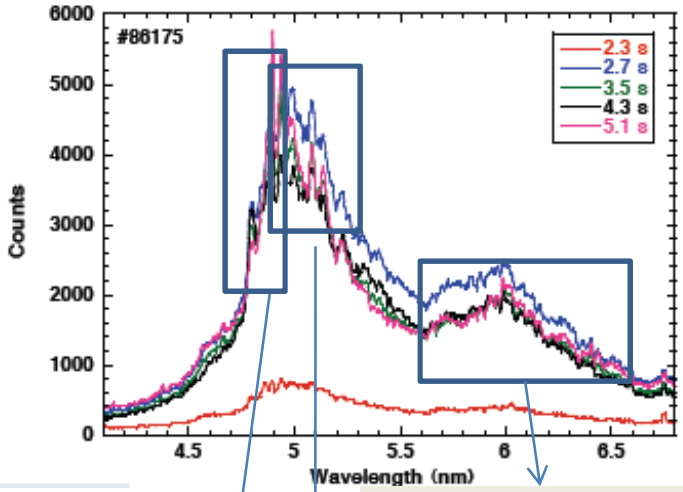

WXXIX-WXLV
$4p_{1/2}$-$4d_{3/2}$

WXXIX-WXLV
$4p_{3/2}$-$4d_{5/2}$

WXXII -WXXVII
4f-5d **& ??**

WXXIX- WXXXVIII $4p^6 4d^n$-$4p^5 4d^{n+1}$ + $4d^{n-1}4f$

WXXVIII-WXX
4d-4f

Conclusions

- Spectrum is dominated by $\delta n = 0$, $n = 4 \leftrightarrow n = 4$ transitions.

- More work needed to understand the origin of 6 nm peak in low temperature spectra.

- No discrete lines will be seen from W XIX – XIII and probably to W XXVII because of the complexity of the spectra; in lower stages the near degeneracy of 4f and 5p binding energies (XIX- XIII), then 4f and 5s (XIV – XVII) and finally the open 4f subshell itself (XVIII – XXVIII).

Special Thanks to:

Chihiro Suzuki , Takako Kato & Daiji Kato NIFS

Funding:

- NIFS
- Science Foundation Ireland

Thank You!

ありがとうございます